Leng et al. *Zool. Res.* 2024, 45(5): 1088−1107
https://doi.org/10.24272/j.issn.2095-8137.2024.037
https://cstr.cn/32248.14.zr.2024.037

ZR | Zoological Research

Article Open Access

Single nucleus/cell RNA-seq of the chicken hypothalamic-pituitary-ovarian axis offers new insights into the molecular regulatory mechanisms of ovarian development

Dong Leng[1,2], Bo Zeng[2], Tao Wang[1], Bin-Long Chen[3,*], Di-Yan Li[1,*], Zhuan-Jian Li[4,*]

[1] *School of Pharmacy*, *Chengdu University*, *Chengdu*, *Sichuan* 610106, *China*

[2] *College of Animal Science and Technology*, *Sichuan Agricultural University*, *Chengdu*, *Sichuan* 611130, *China*

[3] *College of Animal Science*, *Xichang University*, *Xichang*, *Sichuan* 615000, *China*

[4] *College of Animal Science and Technology*, *Henan Agricultural University*, *Zhengzhou*, *Henan* 450046, *China*

ABSTRACT

The hypothalamic-pituitary-ovarian (HPO) axis represents a central neuroendocrine network essential for reproductive function. Despite its critical role, the intrinsic heterogeneity within the HPO axis across vertebrates and the complex intercellular interactions remain poorly defined. This study provides the first comprehensive, unbiased, cell type-specific molecular profiling of all three components of the HPO axis in adult Lohmann layers and Liangshan Yanying chickens. Within the hypothalamus, pituitary, and ovary, seven, 12, and 13 distinct cell types were identified, respectively. Results indicated that the pituitary adenylate cyclase activating polypeptide (PACAP), follicle-stimulating hormone (FSH), and prolactin (PRL) signaling pathways may modulate the synthesis and secretion of gonadotropin-releasing hormone (GnRH), FSH, and luteinizing hormone (LH) within the hypothalamus and pituitary. In the ovary, interactions between granulosa cells and oocytes involved the KIT, CD99, LIFR, FN1, and ANGPTL signaling pathways, which collectively regulate follicular maturation. The SEMA4 signaling pathway emerged as a critical mediator across all three tissues of the HPO axis. Additionally, gene expression analysis revealed that relaxin 3 (RLN3), gastrin-releasing peptide (GRP), and cocaine- and amphetamine regulated transcripts (CART, also known as CARTPT) may function as novel endocrine hormones, influencing the HPO axis through autocrine, paracrine, and endocrine pathways. Comparative analyses between Lohmann layers and Liangshan Yanying chickens demonstrated higher expression levels of *GRP*, *RLN3*, *CARTPT*, *LHCGR*, *FSHR*, and *GRPR* in the ovaries of Lohmann layers, potentially contributing to their superior reproductive performance. In conclusion, this study provides a detailed molecular characterization of the HPO axis, offering novel insights into the regulatory mechanisms underlying reproductive biology.

Keywords: Chickens; Single nucleus/cell transcriptome; Hypothalamic-pituitary-ovarian axis; Signal crosstalk; Hormones

INTRODUCTION

The hypothalamic-pituitary-ovarian (HPO) axis in vertebrates functions as an integrated neuroendocrine system, precisely modulating reproductive signals through positive and negative feedback mechanisms (Mikhael et al., 2019; Zhao et al., 2023). This axis is fundamental in the regulation of ovarian development and reproductive function. Gonadotropin-releasing hormone (GnRH) was among the earliest hypothalamic-releasing hormones to be sequenced and characterized (Conn & Crowley, 1994; Millar, 2005). It is now widely acknowledged that GnRH is synthesized by a specialized subset of hypothalamic neurons, which release the hormone in a pulsatile manner into the hypophyseal portal circulation, directing it to the anterior pituitary (Maggi et al., 2016). The pituitary gland, a pivotal component of the endocrine system, governs various physiological processes, including stress responses, growth, reproduction, and metabolism. Within the pituitary, GnRH, originating from hypothalamic neurons, regulates the synthesis and release of the gonadotropins follicle-stimulating hormone (FSH) and luteinizing hormone (LH) by gonadotrophs (Gona). These hormones share a common glycoprotein α-subunit (CGA) and hormone-specific β-subunit (FSHB and LHB) (Edwards & Raetzman, 2018; Zhu et al., 2007).

Signals from the hypothalamus and pituitary act upon the

Received: 24 May 2024; Accepted: 17 June 2024; Online: 18 June 2024

Foundation items: This work was supported by the Natural Science Foundation of Sichuan Province (2022NSFSC1767) and National Natural Science Foundation of China (32360828)

*Corresponding authors, E-mail: binlong2369@163.com; lidiyan860714@163.com; lizhuanjian@163.com

theca and granulosa cells (GC) of the ovary, precisely regulating their secretion of hormones, including progesterone (P_4) and estradiol (E_2) (Hsueh et al., 2015; Zhao et al., 2023). These ovarian hormones, in turn, influence the synthesis and release of hormones in the hypothalamus and pituitary (Devillers et al., 2022). As a crucial aspect of ovarian function, follicular maturation relies on close interactions between the oocyte and surrounding somatic cells for normal maturation and function (Li & Albertini, 2013; Zhang et al., 2018). Hormonal signaling within the HPO axis plays a pivotal role in regulating these cellular interactions (Li et al., 2021; Ludwig et al., 2023).

To unravel the regulatory mechanisms of the HPO axis, it is crucial to identify the specific cell types and their gene transcription profiles. The advent of single-cell RNA sequencing (scRNA-seq) has revolutionized the study of complex biological systems, enabling high-resolution analysis at the single-cell level. For instance, Kim et al. (2022) identified distinct markers for major subdivisions of the developing chick hypothalamus, providing a valuable framework for understanding the organization of this nascent brain region. However, the precise cellular composition of the chicken (*Gallus gallus*) hypothalamus remains largely unknown. Zhang et al. (2021) constructed a comprehensive cellular transcriptomic atlas of the adult chicken anterior pituitary, identifying four distinct endocrine cell clusters. Nonetheless, research in humans and mice has demonstrated the presence of additional cell populations, including proliferating (Pro) and stem cells, within the pituitary (Lopez et al., 2021; Zhang et al., 2020). Estermann et al. (2020) further detailed cell-lineage specification during gonadal sex differentiation in the chicken embryo. Despite this, the extent to which specific cell types in the adult chicken ovary undergo differentiation and development and whether these cellular compositions and functions exhibit significant variation remain unclear.

Cells in the hypothalamus and pituitary that exceed 50 μm in diameter present considerable challenges for capture via microfluidic droplet generators, impeding gene transcription profiling of tissue-derived neurons using scRNA-seq methods. To overcome this limitation, single-nucleus RNA-seq (snRNA-seq) has emerged as a tool for probing oversized cells or complex tissues that cannot be easily isolated. This approach enables the comprehensive transcriptional profiling of both neuronal and non-neuronal cells within the hypothalamus and pituitary, serving as a powerful tool for investigating neuronal functions and interactions in complex tissues, as well as elucidating the regulatory mechanisms governing the HPO axis.

The Lohmann layer (LM) is widely recognized as a superior egg-laying breed, known for its high egg production and consistent performance. In contrast, the Liangshan Yanying chicken (YY), a well-regarded dual purpose breed in China, is characterized by rapid growth, good stress resistance, and excellent meat quality. However, there is considerable room for improvement in egg production, with Liangshan Yanying chickens producing 110–140 eggs annually, about half the output of Lohmann layers (295–305 eggs). Chen et al. (2021) identified various genes (*GPR65*, *PLPP4*, and *RORB*) potentially linked to oviposition by comparing the transcriptional profiles of follicles at different developmental stages in Lohmann layers and Jilin Black chickens and found that the neuroactive ligand-receptor interaction and cAMP signaling pathways may affect ovarian follicular development. Similarly, Sun et al. (2023) highlighted the critical roles of *ROBO2* and *PRKG2* in follicular selection and preovulatory hierarchy in hens. Wang et al. (2023) performed whole transcriptome sequencing of ovarian tissues from Lohmann layers and Chengkou Mountain chickens and identified three long non-coding RNAs (lncRNAs) targeting *HSD3B1*, *NR5A2*, and *INHBA*, respectively, which may be involved in gonadal development and hormone regulation.

In the current study, we focused on commercial laying hens (Lohmann layers) and local chicken breeds (Liangshan Yanying chickens). We assembled the most extensive transcriptome dataset of the adult chicken HPO axis to date, covering all three primary components. Based on this dataset, we revealed a previously underappreciated level of cellular complexity within the HPO axis. Notably, we identified 17 neuronal subtypes, four Gona subtypes, and seven GC subtypes within the hypothalamus, pituitary, and ovary, respectively, each displaying distinct transcriptional profiles. Furthermore, we mapped the gene transcription patterns of these subtypes, constructing a comprehensive network of interactions among them and with other cellular clusters. Overall, these findings provide a deeper understanding of the cellular complexity and gene regulatory networks involved in reproduction. Understanding these regulatory mechanisms in avian ovarian development is conducive to enhancing the reproductive performance of birds and further improving the egg-laying performance of poultry.

MATERIALS AND METHODS

Ethics statement

The Institutional Animal Care and Use Committee of Sichuan Agricultural University reviewed and approved this animal study (permit No. 2021202046).

Tissue dissociation and preparation

In the autumn of 2022, 200-day-old hens were purchased and transported to Sichuan Agricultural University for dissection and sample collection. The Lohmann layers and Liangshan Yanying chickens were purchased from Xichang Huaning Agricultural and Animal Husbandry Science and Technology Co. Ltd., Liangshan Yi Autonomous Prefecture, Sichuan Province, China. Healthy hens were euthanized by cervical dislocation and perfused with ice-cold phosphate-buffered saline (1×PBS) (HyClone, USA) to eliminate undesired blood cells in target tissues.

Whole brains and ovaries were swiftly dissected and transferred to ice-cold PBS. Subsequently, the hypothalamus and pituitary were manually dissected under a dissecting microscope, snap-frozen in liquid nitrogen, and stored at −80°C for further nuclear isolation. When ovarian samples were collected, yellow and white follicles less than 8 mm in diameter were retained, and larger hierarchical follicles containing more yolk were removed. Fresh tissue was then placed in ice-cold Hanks' Balanced Salt Solution (HBSS) (HyClone, USA) and washed three times. Ovarian tissues were then cut into 1–2 mm pieces and digested with 2 mL of sCelLive™ tissue dissociation solution (Singleron PythoN™ Automated Tissue Dissociation System, Singleron, China) for 15 min at 37℃. Following digestion, samples were filtered through a 40 μm sterile filter, and the filtrate was centrifuged at 1 000 r/min for 5 min at 37°C. The resulting supernatant was

discarded, and the cells were resuspended in 1 mL of PBS. Subsequently, 2 mL of red blood cell lysis solution (Singleron, China) was added at 25°C for 10 min. The solution was then centrifuged at 500 ×*g* for 5 min at 37°C, and the cells were resuspended with 1 mL of PBS. Finally, cells were stained with 0.4% Trypan Blue Solution (Sigma, USA), and cell activity and concentration were assessed under a microscope.

Isolation and sorting of nuclei from hypothalamic and pituitary tissues

Hypothalamic and pituitary tissues from chickens stored at −80°C, were initially washed with pre-cooled PBSE (PBS buffer with 2 mmol/L EGTA). Nuclei were then isolated utilizing GEXSCOPE® Nucleus Separation Solution (Singleron Biotechnologies, China) in accordance with the manufacturer's guidelines. The isolated nuclei were resuspended in PBSE to a concentration of 1×10^6 nuclei per 400 μL, then filtered through a 40 μm cell strainer and enumerated using Trypan blue. 4',6-Diamidino-2-phenylindole (DAPI) staining (1:1 000) (Thermo Fisher Scientific, USA) was applied to PBSE-enriched nuclei, with DAPI-positive nuclei identified as singlets.

Construction and sequencing of single nucleus/cell libraries

Transcriptional profiles for the hypothalamus and pituitary were generated using snRNA-seq, while scRNA-seq was employed for the ovary. The single-nucleus and single-cell suspensions were first adjusted to 3×10^5–4×10^5 nuclei/mL and 1×10^5 cells/mL in PBS, respectively. Subsequently, these suspensions were loaded onto a microfluidic chip (GEXSCOPE® Single Nucleus RNA-seq Kit/GEXSCOPE™ Single-Cell RNA Library Kit, Singleron, China). Library construction for snRNA-seq/scRNA-seq followed the manufacturer's instructions (Singleron, China). The resulting libraries were sequenced on an Illumina HiSeq×10 instrument (Illumina, USA), generating 150 bp paired-end reads.

Processing of single nucleus/cell RNA sequencing data

Raw sequencing data were processed using the CeleScope v.1.14.0 pipeline (https://github.com/singleron-RD/CeleScope). Reads were aligned to a reference genome (Ensemble assembly: bGalGal1. mat. broker. GRCg7b) to generate count matrices. These matrices and associated metadata were imported into the Seurat package v.4.4.0 in R for further analysis, with default parameters applied unless specified otherwise (Butler et al., 2018). To ensure data quality, nuclei or cells expressing fewer than 200 genes and genes detected in fewer than 100 nuclei or cells were excluded. The aligned reads were filtered to obtain cell barcodes and unique molecular identifiers (UMI) for gene-cell matrices. Gene expression values were normalized and scaled using the NormalizeData and ScaleData functions. Principal component analysis (PCA) was performed on the top 2 000 variable genes identified by the FindVariableFeatures function. The top 30 principal components were selected for subsequent analyses, determined by the JackStraw and ElbowPlot functions. Finally, integration of the Lohmann layer and Liangshan Yanying chicken datasets was achieved using the FindIntegrationAnchors and IntegrateData functions.

Identification of cell clustering and cell type

Cell clusters were identified using the Louvain algorithm, implemented through the FindClusters function in Seurat. To ensure accurate clustering resolution, the relationship between clusters was visualized at multiple resolutions using the clustree package v.0.5.0 (Zappia & Oshlack, 2018). Based on these results, the resolutions for the hypothalamus, pituitary, and ovary were determined to be 0.4, 0.5, and 0.5, respectively. The Unified Manifold Approximation and Projection for Downscaling Reduction (UMAP) (McInnes et al., 2018) approach was used to calculate 2D dimensionality reduction for all sequencing libraries. The resulting clusters were classified into distinct cell types and annotated using numerous typical cell type markers reported in the literature. Cell type-specific gene expression profiles were identified using the FindAllMarkers function, with criteria for identification set at an absolute $\log_2$ fold change (FC)≥0.25 and a minimum cell population fraction of 0.25 in either of the two populations. Finally, Seurat was employed to generate feature, violin, and dot plots.

Identification of differentially expressed genes (DEGs) and gene function analysis

DEGs in the hypothalamus, pituitary, and ovary of Lohmann layers and Liangshan Yanying chickens were identified using the FindMarkers function in Seurat. DEG sets meeting the thresholds ($|\log_2FC|>0.25$, $P<0.05$, and P-adjusted<0.01) were subjected to Gene Ontology (GO) and Kyoto Encyclopedia of Genes and Genomes (KEGG) functional enrichment analysis using the clusterProfiler package v.4.9.2 in R, based on the hypergeometric distribution principle (Wu et al., 2021). The results were visualized using bar and dot plots.

Pseudotime analysis

Pseudotime trajectories for all GC subtypes in the ovary were constructed using Monocle3 v.1.3.1 (Cao et al., 2019). This approach sorts single cells along a trajectory based on the similarity of their gene expression patterns, effectively modeling cellular dynamics over time. The spatial co-expression of genes was assessed by calculating Moran's Index (Moran's I) to construct pseudotime trends in gene expression.

Cell-cell communication inference

To comprehend the global patterns of cell-to-cell communication within the chicken hypothalamus, pituitary, and ovary, and to uncover the signaling events associated with successive cell lineages, the R package CellChat v.1.6.1 was utilized, with ligand-receptor interactions for visual intercellular communications from snRNA-seq/scRNA-seq data (Jin et al., 2021). As the database primarily covers human genes, homologous chicken genes were selected based on their relationships with human counterparts.

Gene expression analysis by *in situ* hybridization

Brains, pituitary glands, and ovaries (with follicles larger than 8 mm in diameter removed) were collected from 200-day-old Lohmann layers and Liangshan Yanying chickens and fixed overnight in 4% paraformaldehyde in DEPC-PBS (Servicebio, China). Following fixation, tissue blocks were cut to a thickness of approximately 3 mm in a fume hood, dehydrated through an alcohol gradient, rendered transparent with xylene, and embedded in wax. Paraffin block slices (4 μm thick) were prepared using a microtome, processed through BioDewax and Clear solutions (Servicebio, China), dehydrated in ethanol, soaked in alcohol, and rinsed in DEPC water. Protease K digestion was performed at 37°C, followed by natural cooling. Pre-hybridization at 37°C was conducted prior to overnight hybridization with probes (Supplementary Table

S1). After hybridization, the slices were washed in SSC buffers and blocked with serum, then incubated with anti-DIG-APBCIP/NBT solution (Servicebio, China) at 4°C for 12 h for microscopic observation, counterstained with DAPI, air-dried, and sealed with Glycerol Jelly Mounting Medium.

Production data collection

Production data for Lohmann layers were obtained from Xichang Huaning Agricultural and Animal Husbandry Science and Technology Co. Ltd., Liangshan Yi Autonomous Prefecture, Sichuan Province, China. Production data for Liangshan Yanying chickens were obtained from Meigu Flying Eagle Yanying Chicken Breeding Family Farm, Liangshan Yi Autonomous Prefecture, Sichuan Province, China. Each chicken was individually caged, and data were recorded according to its unique wing tag.

Statistical analysis

Statistical analysis of egg-laying traits for Lohmann layers and Liangshan Yanying chickens was performed using the Wilcoxon test with the ggpubr package v.0.6.0 in R (https://CRAN.R-project.org/package=ggpubr). Differences were considered significant at $P<0.05$.

RESULTS

Transcriptional clustering of cell populations in all three HPO axis tissues

To explore the regulatory functions of the HPO axis at the cellular level, tissues from the hypothalamus, pituitary, and ovary were collected from adult Lohmann layers and Liangshan Yanying chickens. Subsequently, snRNA-seq was performed on two isolated hypothalamus and two pituitary samples, while scRNA-seq was performed on two isolated ovary samples (Figure 1A; Supplementary Figure S1A). High-quality nuclei or cells were selected based on the total number of expressed genes and UMIs in each nucleus or cell, and the percentage of UMIs mapped to mitochondrial genes relative to total genes (Supplementary Figure S1B–G). This approach yielded 26 975 nuclei from the hypothalamus, 25 664 nuclei from the pituitary, and 17 408 cells from the ovary for subsequent analyses. To classify major cell clusters, canonical correlation analysis was conducted on the gene expression matrix, followed by integration of both chicken datasets using UMAP. This analysis identified 23 major cell clusters in the hypothalamus (Figure 1B), 19 in the pituitary (Figure 1C), and 27 in the ovary (Figure 1D), each exhibiting distinct transcriptional profiles.

Identification of cell types in all three HPO axis tissues

To delineate the cellular populations present in the hypothalamus, pituitary, and ovary, DEG analysis was performed for all clusters in each tissue separately. The top 10 marker genes for each cluster were visualized in a heatmap (Supplementary Figure S2A–C). Hierarchical clustering was applied using the 50 most variably expressed genes per cluster (Figure 2A–C) and Spearman correlation coefficients were calculated based on the expression matrices of the 1 000 genes with the largest standard deviation in each tissue (Supplementary Figure S2D, E).

Based on the expression patterns of pan-neuronal markers *SNAP25* and *SYT1*, 23 cell clusters in the hypothalamus were categorized into seven cell types, including 17 neuronal and six non-neuronal clusters (Chen et al., 2017) (Figure 2D; Supplementary Figure S3A). Among the neuronal clusters, 10 were classified as glutamatergic subtypes (nGlut1–nGlut10, clusters 4, 6, 8, 10, 11, 13, 16, 17, 21, and 22) and five as GABAergic subtypes (nGABA1–nGABA5, clusters 2, 3, 12, 14, and 18) based on their distinct expression of *SLC17A6* and *SLC32A1* (Chen et al., 2017). The two remaining neuronal clusters exhibited low expression of both *SLC17A6* and *SLC32A1*. Hierarchical clustering and correlation analysis designated one of the clusters as mixed neurons (nMixed, cluster 0) (Figure 2A; Supplementary Figure S2D) and the other cluster as histaminergic neuron-like cells (Hista-like, cluster 20), the latter characterized by elevated expression of *SLC18A2* (Zhou et al., 2022). The six non-neuronal clusters were further classified into distinct cell types based on their gene expression profiles, including oligodendrocytes (cluster 1, characterized by *PLP1*), astrocytes (cluster 5, characterized by *AGT*), oligodendrocyte progenitor cells (OPCs, cluster 7, marked by *PDGFRA*), microglia (cluster 9, characterized by *SALL1*), ependymal cells (cluster 15, labeled by *DNAH10*), and endothelial cells (cluster 19, identified by *VWF*). Neuronal cells were notably predominant in the hypothalamus, constituting 71.66% of the cellular population (Supplementary Figure S3B). Enriched GO functional terms associated with these neuronal cells included “axon guidance” and “regulation of trans-synaptic signaling” (Supplementary Figure S3C), while enriched KEGG pathways included “axon guidance” and “neuroactive ligand-receptor interaction” (Supplementary Figure S3D).

In the pituitary, 12 distinct cell types were identified, including five classical pituitary endocrine cell populations and seven other cell populations. Based on known marker genes for pituitary endocrine cell lineages, clusters 0, 2, and 17 corresponded to lactotrophs (Lac, characterized by high prolactin (*PRL*) expression); cluster 1 corresponded to corticotrophs (Cort, characterized by high *POMC* expression); clusters 3 and 6 corresponded to somatotrophs (Soma, characterized by high *GH* expression); clusters 4, 5, 10, and 11 corresponded to Gona (characterized by high *PGR* and *FSHB* expression); and cluster 8 corresponded to thyrotrophs (Thy, characterized by high *TSHB* expression) (Figure 2E; Supplementary Figure S4A). Among the seven other cell populations, cluster 7 was defined as stem cells (exhibiting high *LHX3* expression and low *SOX2* expression; cluster 9 was classified as endothelial cells (with high *EMCN* expression; clusters 12 and 16 were identified as Pro cells (with high expression of *GATA2* and *ISL1* markers); cluster 13 was classified as macrophages (with higher *PTPRC* expression compared to cluster 14); cluster 14 was defined as microglia (with higher *DOCK2* expression); cluster 15 was classified as fibroblasts (with high expression of *CFD*); and cluster 18 was identified as posterior pituitary cells (PPCs, with high *COL25A1* expression). In this analysis, Lac emerged as the most prevalent cell population in the pituitary, constituting 28.11% of the total, followed by Gona (20.5%), Cort (16.12%), and Soma (14.27%) cells (Supplementary Figure S4B). Identification of these cell types through specific marker genes revealed distinct enrichment in GO terms and KEGG pathways that align with their biological functions (Supplementary Figure S4C, D).

The 27 clusters identified in the ovary were further categorized into 13 distinct cell types. Cluster 0 was identified as early theca cells (characterized by elevated *OGN* expression); cluster 1 was identified as stromal cells

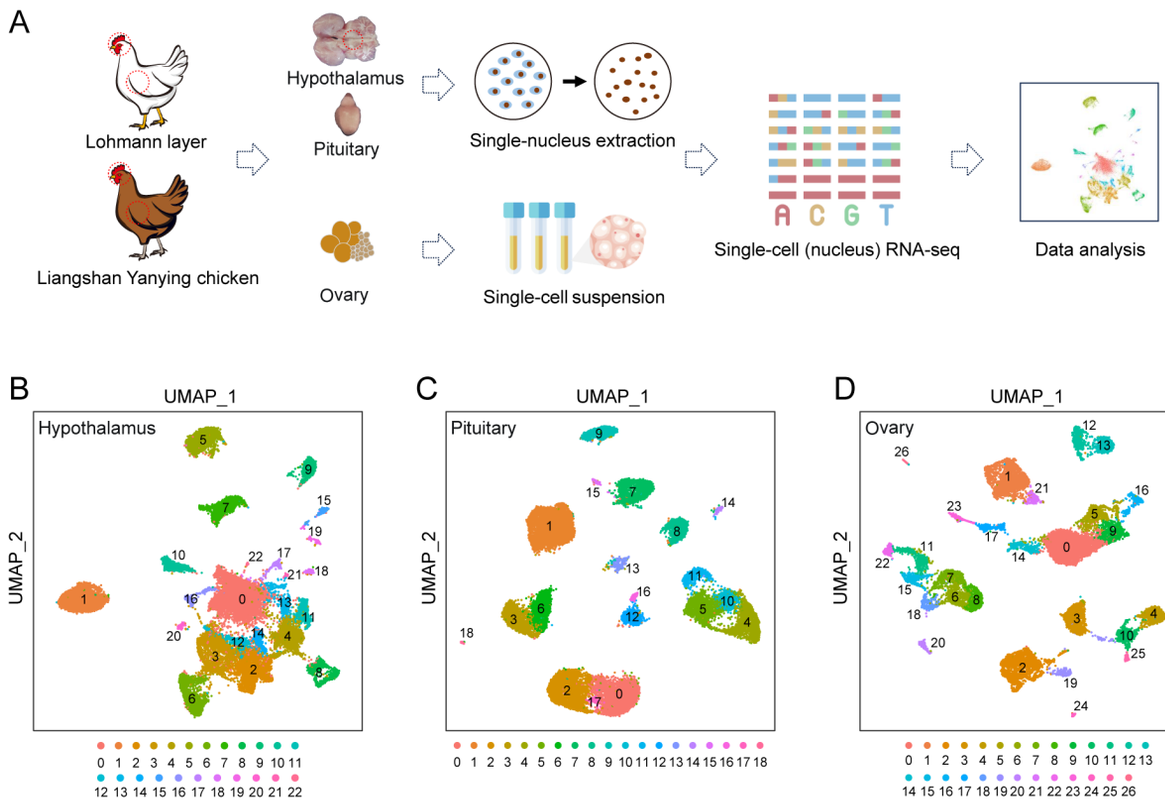

Figure 1 Transcriptional clustering of cell populations in all three HPO axis tissues

A: Flowchart overview of snRNA-seq of the hypothalamus and pituitary and scRNA-seq of the ovary in Lohmann and Liangshan Yanying chickens. Specific steps included sample collection, single-cell nucleus extraction/single-cell suspension preparation, library construction, sequencing, and data analysis. B–D: UMAP visualization of all cells after quality control in the hypothalamus, pituitary, and ovary.

(characterized by high *POSTN* and *DCN* expression); clusters 2 and 19 represented macrophages (marked by *CD74* expression); cluster 3 denoted B cells (with high *JCHAIN* expression); clusters 4, 10, 24, and 25 corresponded to T/natural killer (NK) cells (characterized by *CD3D* expression); clusters 5 and 16 were classified as smooth muscle cells (expressing *TAGLN*); clusters 6, 7, 8, 11, 15, 18, and 22 were identified as GCs (with high anti-Mullerian hormone (*AMH*) expression); cluster 9 was classified as fibroblast-like stromal cells (expressing both stromal cell markers *POSTN* and *DCN* and fibroblast marker *COL1A1*); clusters 12, 13, and 26 represented endothelial cells (characterized by elevated *VWF* expression); cluster 14 comprised erythroblasts (marked by *HBAD* expression); clusters 17 and 23 were identified as secretory-theca cells (characterized by *OGN* and hormone-related genes like gastrin-releasing peptide (*GRP*); cluster 20 represented oocytes (characterized by high *ZP3* expression); and cluster 21 was identified as pre-GCs (characterized by elevated *CYP19A1* expression) (Figure 2F; Supplementary Figure S5A). As expected, GCs constituted the most prevalent cell type in the ovary, representing 19.85% of the total cell population, followed by early theca cells (18.45%) and stromal cells (11.2%) (Supplementary Figure S5B). Each cell type demonstrated specific enrichment in GO terms and KEGG pathways corresponding to their respective biological functions (Supplementary Figure S5C, D).

Molecular and cellular signatures of different neuronal subtypes and cellular crosstalk with glial cells in the hypothalamus

To elucidate the subtypes of hypothalamic neurons involved in regulating the HPO axis and the mechanisms governing their interactions, neuronal clusters identified through cluster analysis were further analyzed. The initial cellular annotations did not conclusively identify specific neuronal types within the nMixed and Hista-like clusters, and the nGlut10 cluster potentially represented a non-hypothalamic cell cluster (Figure 2A; Supplementary Figure S2D). Consequently, these three neuronal clusters were excluded, and the remaining nine glutamatergic and five GABAergic neuronal subtypes were visualized using UMAP (Figure 3A). Potential subtype-specific marker genes were identified for each of the 14 neuronal clusters. Notably, most clusters exhibited subtype-specific genes unique to their respective clusters, with some clusters defined by the combinatorial expression of multiple marker genes (Figure 3B). The expression of particular neuropeptides and receptors distinguished several neuronal subtypes. For instance, luteinizing hormone receptor (*LHCGR*) and oxytocin (*OXT*) were identified as potential markers for the nGlut3 and nGlut6 cell clusters, respectively.

The distinct expression of neuropeptides in specific neuronal subtypes determines the signals transmitted by these cells, while the expression of specific neuropeptide receptors indicates the ability of these cells to receive particular signals. Evaluation of the expression profiles of various neuropeptides and receptors across different hypothalamic neuronal subtypes revealed a highly diverse expression pattern (Supplementary Figure S6). Most neuropeptide and receptor genes implicated in HPO axis regulation were predominantly expressed in only one or a few neuronal subtypes, consistent with observations in humans and mice (Chen et al., 2017; Zhou et al., 2022). Furthermore,

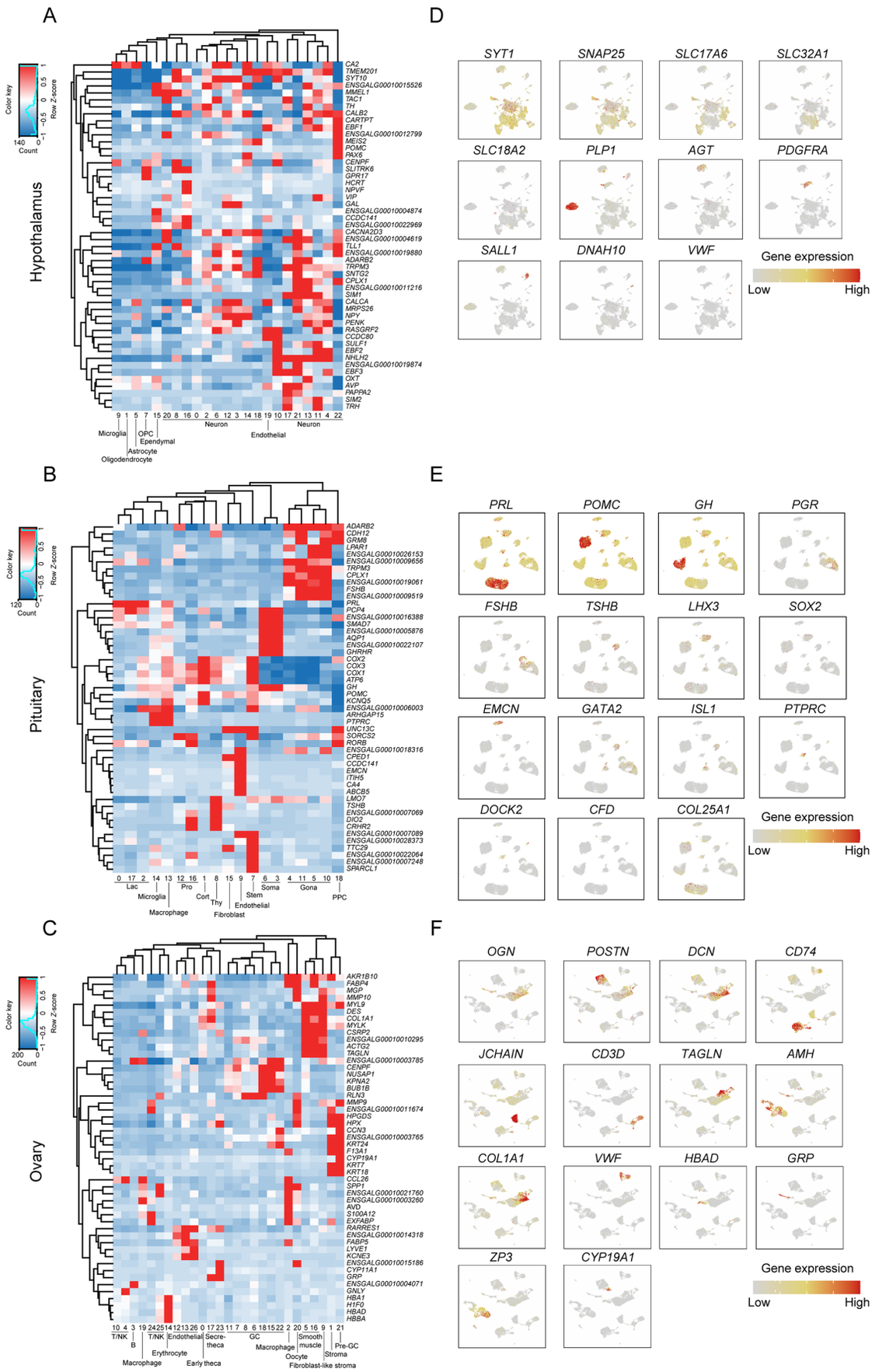

Figure 2 Identification of cell types in all HPO axis tissues

A–C: Heatmap and hierarchical clustering based on expression of the top 50 most variable genes in the hypothalamus, pituitary, and ovary. D–F: UMAP plot showing gene expression characterizing all cell types in the hypothalamus, pituitary, and ovary.

our analysis revealed that co-expression of multiple neuropeptides and receptors was a common feature among many hypothalamic neurons, suggesting their involvement in complex feedback regulation within the HPO axis. For instance, the nGlut2 cluster showed high expression of *ADCYAP1* and *ESR2*; the nGlut3 cluster showed high expression of *GHRH*, *FSHR*, *GRPR*, and *LHCGR*; and the nGlut8 cluster showed high expression of *CRH*, *TRH*, *CRHR2*, *ESR1*, and *GHR*. These findings indicate complex crosstalk among diverse peptide signaling pathways, with hormones from the pituitary and ovary influencing the synthesis and release of various neuropeptides in the hypothalamus through feedback regulation.

To further explore this crosstalk between neuronal subtypes, we focused on the nGABA1 cluster with high *GNRH1* expression (Supplementary Figure S6A). In this analysis, a total of 143 ligand-receptor pairs were identified across 14 neuronal clusters, which were further categorized into 48 signaling pathways. The nGABA1 cluster emerged as a key communication "hub" within these networks (Figure 3C; Supplementary Figure S7A, B and Table S2). Through communication pattern analysis, four patterns were identified in outgoing secretory cells and two in incoming target cells (Figure 3D, E). The 48 signaling pathways were also grouped into four categories based on functional or structural similarities (Figure 3F; Supplementary Figure S7C). Based on network centrality analysis, the nGABA1 cluster was identified as a major ligand source in the SEMA4 pathway, prominently expressing the *SEMA4D* ligand gene. The nGlut3 cluster, which also expressed a variety of receptor genes related to negative feedback regulation between the hypothalamus and pituitary, was also identified as a major target, expressing the *PLXNB2* receptor gene (Figure 3G; Supplementary Figure S7D, E) (Giacobini et al., 2008; Saha et al., 2012). In addition, the nGABA1 cluster was found to be a primary target in the pituitary adenylate cyclase activating polypeptide (PACAP) signaling pathway (Figure 3H; Supplementary Figure S7F) (Halvorson, 2014), indicating a complex regulatory relationship among hypothalamic neurons.

To explore the signaling interactions between GnRH neurons and glial cells, the expression profiles of neuropeptides and receptors were analyzed in the nGABA1 cluster and various glial cells. Most neuropeptides were either absent or poorly expressed in glial cells (Supplementary Figure S8A). However, *GRPR* and *RXFP1* were highly expressed in astrocytes, *GHR* and *LHCGR* were highly expressed in OPCs, and *FSHR* was highly expressed in microglia. These findings suggest that the activities of these glial cells are also regulated by multiple pituitary hormones (Supplementary Figure S8B). Crosstalk analysis demonstrated that the nGABA1 cluster had the most active interactions with astrocytes and OPCs (Supplementary Figure S8C). Specifically, astrocytes and OPCs targeted the nGABA1 cluster through the VTN, AGT, and SEMA3 pathways, while the nGABA1 cluster targeted both through the SEMA4 pathway (Supplementary Figure S8D). These results suggest a tightly coordinated interaction between glial cells, especially astrocytes, and neuronal populations in the hypothalamus that synthesize and release GnRH.

Molecular and cellular signatures of different Gona subtypes and cellular crosstalk with other cell types in the pituitary

Distinct Gona subtypes within the pituitary exhibit notable differences in hormone synthesis and secretion, likely driven by subtype-specific gene expression and regulatory mechanisms. Our analysis identified four Gona subtypes, which were visualized through UMAP (Figure 4A). Subsequent DEG analysis further revealed unique marker genes for each subtype, with relaxin 3 (*RLN3*), *PLXDC2*, *HPGDS*, and tyrosine kinase ligand (*KITLG*) exhibiting particularly high expression levels in Gona1–Gona4 (Figure 4B). The expression profiles of critical transcription factors, hormone-related genes, and receptor genes in these subtypes were further explored. While certain genes were uniformly expressed across all subtypes, others showed elevated expression in specific subtypes only (Figure 4C). These findings suggest that the regulatory role of the HPO axis in the pituitary is both broad and specific. Notably, luteinizing hormone β-subunit (*LHB*) expression was absent in all four Gona subtypes, while GnRH receptor (*GNRHR*) was predominantly expressed in Gona1 and to a lesser extent in Gona3 (Supplementary Figure S10A). Interestingly, *ESR1* and *PGR* were also highly expressed in these two Gona subtypes, suggesting a potential link to the negative feedback regulation between the ovary and pituitary.

To further elucidate the gene expression and functional distinctions among the Gona subtypes, 143, 189, 120, and 223 unique DEGs were identified in the Gona1–Gona4 clusters, respectively (Figure 4D). GO analysis of these DEGs highlighted enrichments in functional terms consistent with canonical gene expression patterns, as previously described (Figure 4E). These results suggest that the pituitary harbors multiple functionally distinct Gona subtypes, each potentially playing different roles in the overall regulation of the HPO axis.

Previous studies have highlighted the significant interplay between diverse cell types in the pituitary, directly influencing the hormone-secreting activity of various hormone-secreting cells (Perez-Castro et al., 2012; Santiago-Andres et al., 2021). Specifically, hormones secreted by one cell type can modulate the activity and hormone secretion of other cell types, thereby playing a crucial role in overall HPO axis regulation and the maintenance of hormonal homeostasis and normal physiological functions. To further explore the signaling crosstalk between different cell types in the pituitary, the expression levels of ligand-receptor interaction pairs in 12 pituitary cell types were analyzed. In total, 96 ligand-receptor pairs were identified and further categorized into 33 signaling pathways. Among these, the Gona cluster was identified as a key communication "hub" (Figure 5A; Supplementary Figure S9A, B and Table S3).

Following communication pattern analysis, two outgoing and three incoming signaling patterns were identified in secretory and target cells, respectively (Figure 5B, C). Additionally, the 33 signaling pathways were grouped into four categories based on functional or structural similarities (Figure 5D; Supplementary Figure S9C). Our analysis primarily focused on the SEMA4 pathway, previously identified in the hypothalamus, as well as two endocrine signaling pathways related to FSH and PRL. Network centrality analysis revealed that the Gona cluster was involved in the SEMA4 pathway through both autocrine and paracrine secretion, expressing both the ligand gene *SEMA4D* and receptor gene *PLXNB2* (Figure 5E; Supplementary Figure S9D, E). The signaling crosstalk of Gona in the FSH and PRL pathways mainly involved autocrine and paracrine secretion, respectively (Figure 5F, G; Supplementary Figure S9F, G). Interestingly,

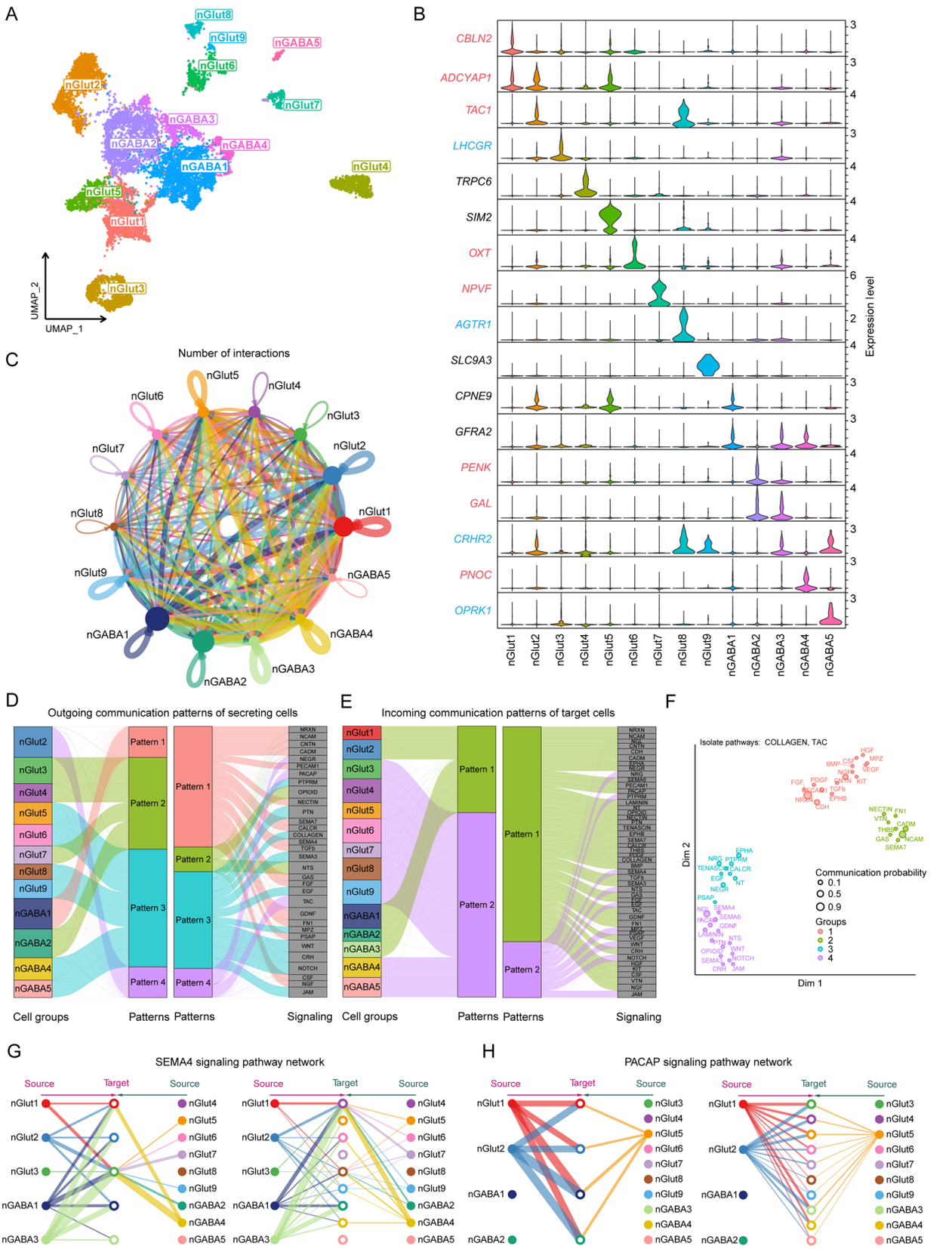

Figure 3 Molecular and cellular signatures of different neuronal subtypes in the hypothalamus

A: UMAP plot showing 14 major neuronal clusters in the hypothalamus. B: Violin plots showing expression of subtype markers in the 14 neuronal clusters. Neuropeptide- (red) and receptor- (blue) related genes are marked with relevant colors. C: Circle plot representing cell communication among neuronal subtypes. Arrows originate from ligand-expressing cells and point toward receptor-expressing cells. Circle sizes represent number of cells, and edge widths represent number of ligand-receptor pairs. D, E: Inferred outgoing and incoming communication patterns in hypothalamic neurons. F: Distribution of signaling pathways with their functional similarities. G, H: Hierarchical plot showing intercellular communication network for SEMA4 and PACAP signaling pathways. Circle sizes represent number of cells, and edge widths represent communication probability.

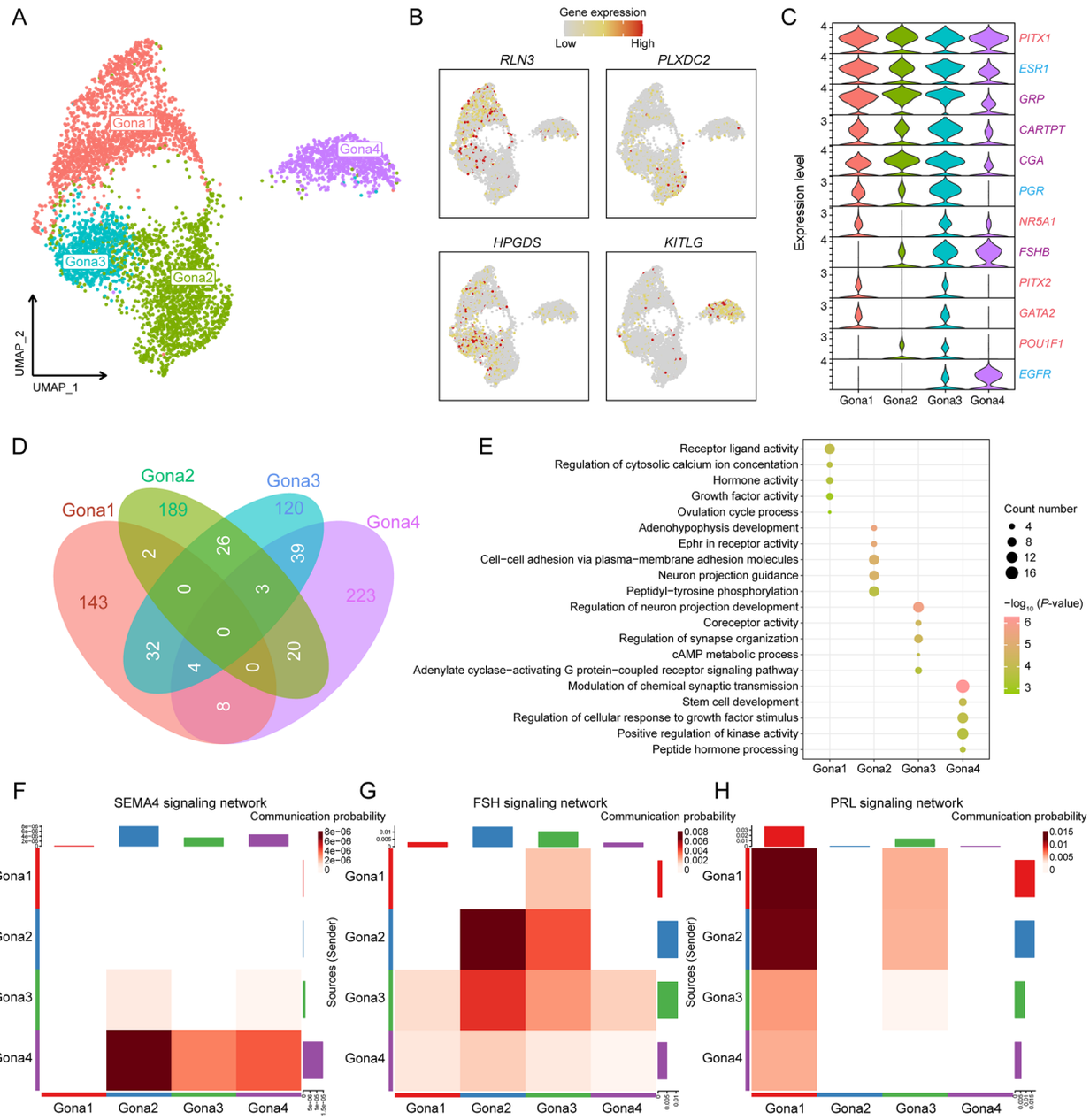

Figure 4 Molecular and cellular signatures of different Gona subtypes in the pituitary

A: UMAP plot showing four Gona subtypes in the pituitary. B: UMAP plot showing expression of representative DEGs for each cluster. C: Violin plots showing expression of important genes in four Gona subtypes. Transcription factor- (red), hormone- (purple), and receptor- (blue) related genes are marked with corresponding colors. D: Venn diagram showing intersection of DEGs between four Gona subtypes and number of unique DEGs for each. E: Dot plots showing GO enrichment analysis of unique DEGs for each Gona subtype. Color indicates *P*-value and circle indicates gene counts. F–H: Heatmap showing intercellular communication networks for SEMA4, FSH, and PRL signaling pathways. Sender cells (ligand sources) are shown on y-axis and receiving cells (receptor expression) are shown on x-axis. Darker colors indicate greater communication probability between two subtypes. Upper and right-hand column bar plots show accumulation of x-axis and y-axis intensities.

the four Gona subtypes demonstrated distinct roles within each of these three pathways (Figure 4F–H; Supplementary Figure S10B–D). These findings support the presence of ultrashort communication between pituitary cell populations (Denef, 2008; Le Tissier et al., 2012), suggesting that gonadotropin synthesis and release in the pituitary are jointly regulated by multiple signals, adding a further layer of complexity to the regulatory functions of the HPO axis.

Molecular and cellular signatures of different GC subtypes in the ovary and signal crosstalk with oocytes

GCs play a pivotal role in follicular development and maturation within the ovary, constituting a crucial component of the HPO axis regulatory system. Unlike mammals, avian species are capable of continuous follicular development, maturation, and smooth ovulation after reaching a specific growth stage (Johnson, 2015). Consequently, the ovaries of breeding birds contain follicles at varying developmental stages, with the GCs within these follicles exhibiting distinct molecular and cellular signatures.

Our analysis identified seven GC subtypes within the ovarian dataset, which were visualized using UMAP (Figure 6A). Subsequently, DEG analysis was performed to

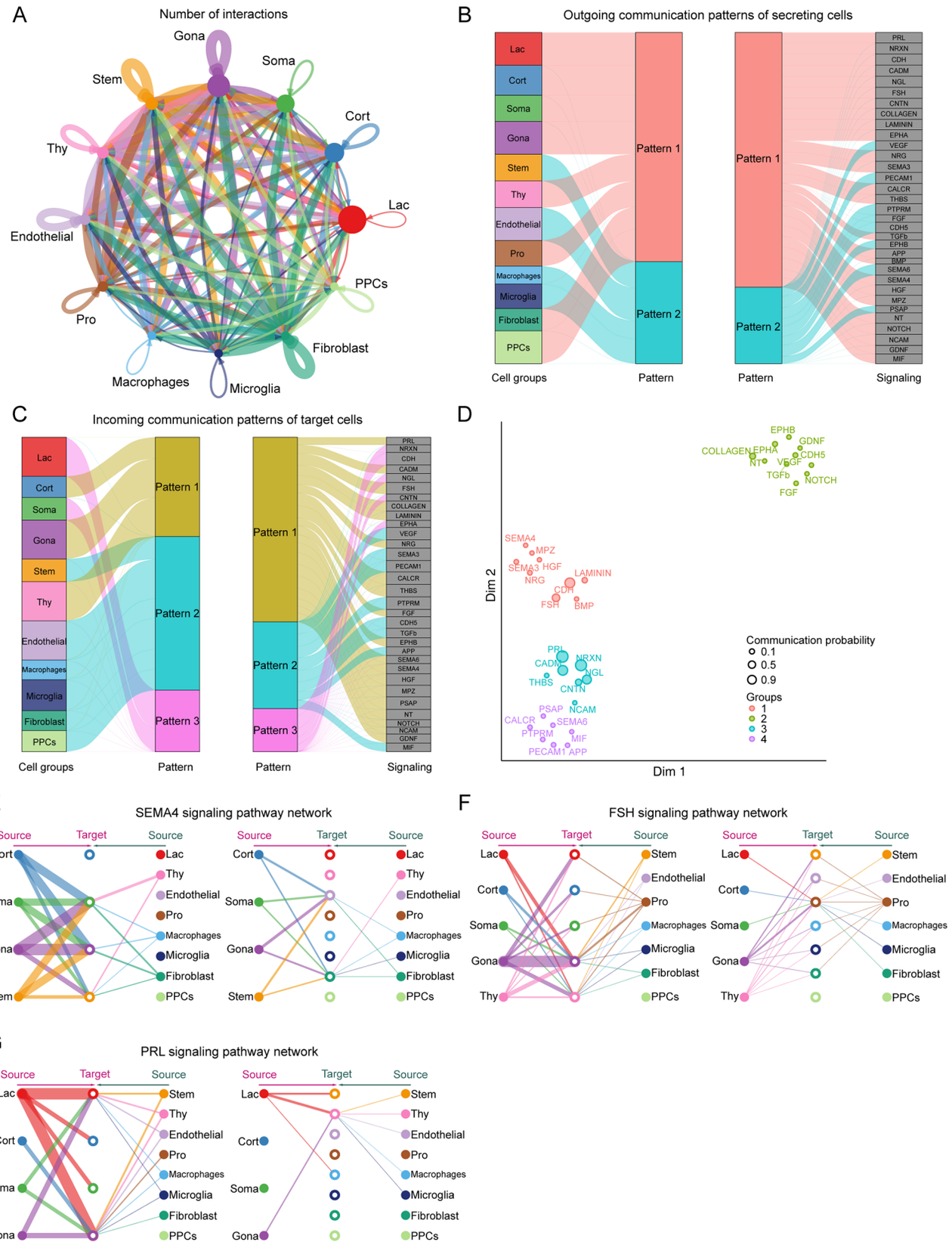

Figure 5 Signal crosstalk between different cell types in the pituitary

A: Circle plot representing cell communication among pituitary cell types. Arrows originate from ligand-expressing cells and point toward receptor-expressing cells. Circle sizes represent number of cells, and edge widths represent number of ligand-receptor pairs. B, C: Inferred outgoing and incoming communication patterns between different cell types in the pituitary. D: Distribution of signaling pathways with their functional similarity. E–G: Hierarchical plot showing intercellular communication networks for SEMA4, FSH, and PRL signaling pathways. Circle sizes represent number of cells, and edge widths represent communication probability.

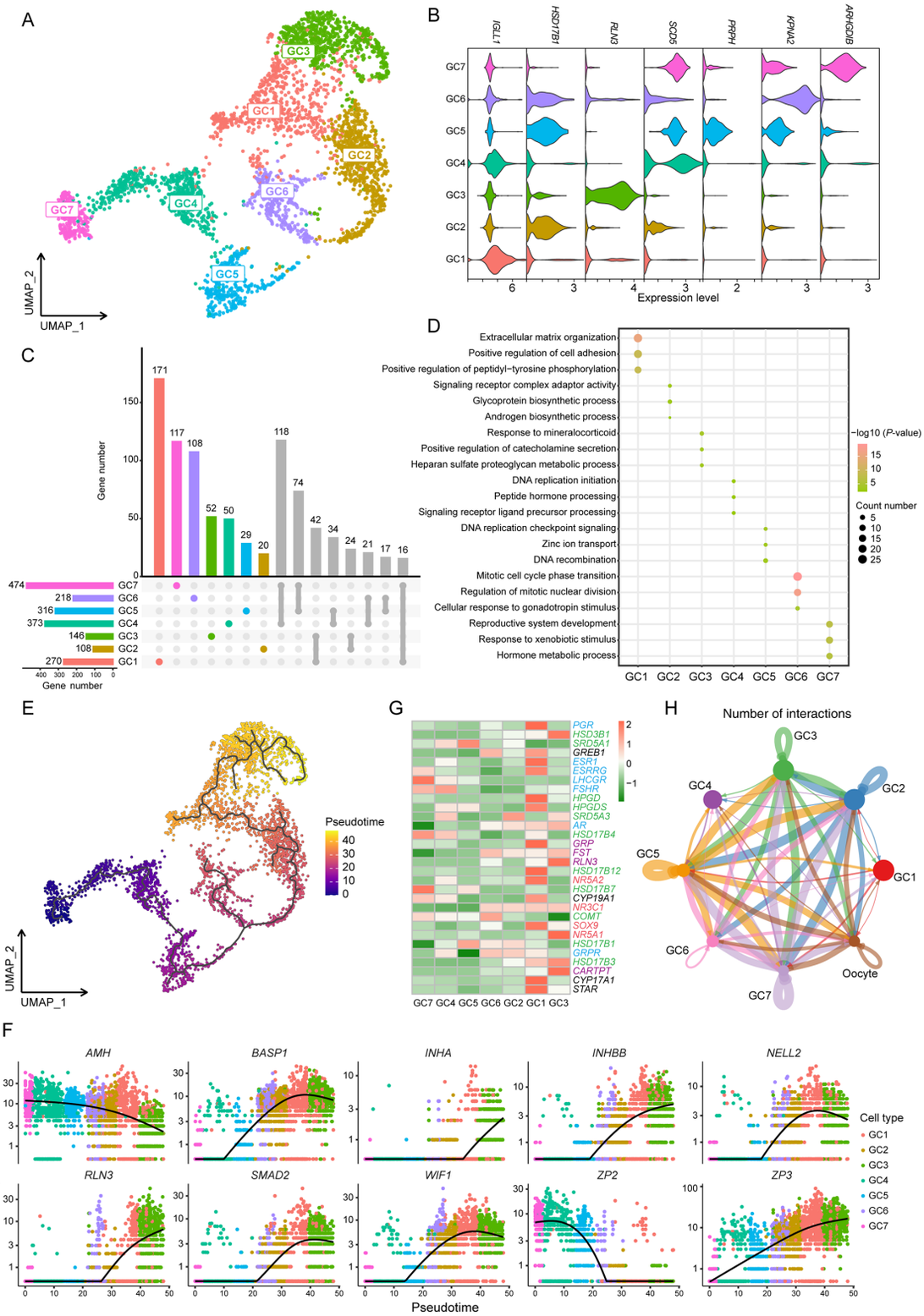

Figure 6 Molecular and cellular signatures of different GC subtypes in the ovary

A: UMAP plot showing seven GC subtypes in the ovary. B: Violin plot showing expression of representative DEGs for each cluster. C: Upset plots of DEGs for seven GC subtypes. Different colored columns at the top (except gray) represent number of unique DEGs for each subtype, respectively. Bottom left histogram shows total number of DEGs in each subtype. D: Dot plots showing GO enrichment analysis of unique DEGs for each GC subtype. Color indicates *P*-value and circle indicates gene counts. E: Monocle trajectory inference tracing a pseudotime path of GC subtypes. F: Visualization of transition of highly expressed genes in pseudotime ordering of GC subtypes. G: Heatmap showing expression of ovarian development-related genes in seven GC subtypes. Transcription factor- (red), enzyme- (green), hormone- (purple), and receptor- (blue) related genes are marked with corresponding colors. H: Circle plot representing cell communication between GC subtypes and oocytes. Arrows originate from ligand-expressing cells and point toward receptor-expressing cells. Circle sizes represent number of cells, and edge widths represent number of ligand-receptor pairs.

select a representative DEG for each subtype (Figure 6B). The count of unique DEGs varied across the GC1–GC7 clusters, ranging from 20 to 171 (Figure 6C). To further explore the functional distinctions among these subtypes, GO enrichment analysis was conducted for these unique DEGs (Figure 6D), revealing that several functional terms related to DNA replication and mitosis were enriched in the GC4–GC6 cluster, suggesting that these subtypes may originate from follicles at different developmental stages.

To investigate this hypothesis, pseudotime trajectory analysis of the seven GC subtypes was performed, using the GC7 cluster as the starting point due to its highest expression of *AMH* (Figure 6E). The results revealed a specific developmental progression, starting from the GC7 cluster and progressing towards the GC3 cluster. This developmental trajectory was further visualized by mapping the sequential dynamics of gene expression (Figure 6F). Intriguingly, *RLN3*, highly expressed in the nGABA3 cluster of the hypothalamus and Gona1 cluster of the pituitary, exhibited a gradual up-regulation along the GC pseudotime trajectory, reaching peak expression in the GC3 cluster (Figure 4B; Supplementary Figure S6A).

Given the molecular and functional diversity among the seven GC subtypes, variations in gene expression related to ovarian development were examined (Figure 6G). Interestingly, *LHCGR* and *FSHR* showed high expression exclusively in the GC7 and GC4 clusters at the early stages of the pseudotime trajectory, while hormones such as *GRP*, *RLN3*, and cocaine and amphetamine regulated transcript (*CARTPT*, also named *CART*) were predominantly expressed in GC1 and GC3 at the later stages of the trajectory. Additionally, transcription factors influencing GC proliferation, differentiation, and hormone synthesis, such as *NR3C1* and *NR5A1*, exhibited elevated expression primarily in GC3 at the end stage of the trajectory. These findings suggest that the regulation of ovarian development by the HPO axis is both directed and staged, with distinct transcriptional regulatory mechanisms active at different developmental stages, potentially linked to variations in hormone levels and regulatory factors within the HPO axis.

Further analysis of intercellular communication among the 13 cell types in the ovary indicated that the GC and oocyte clusters served as primary communication “hubs” (Supplementary Figure S11A). Network centrality analysis of the SEMA4 pathway, also identified in the hypothalamus and pituitary, highlighted GCs as both primary ligand sources and target cells (Supplementary Figure S11B). To gain deeper insights into the interaction between GCs and oocytes, the expression levels of ligand-receptor interaction pairs in the seven GC subtypes and oocyte clusters were examined (Figure 6H; Supplementary Figure S11C, D and Table S4). This analysis revealed that the GC2 and GC3 clusters, which appeared later in the pseudotime trajectory, engaged in a broad range of autocrine and paracrine interactions (Figure 7A; Supplementary Figure S11E). The primary mediators of the SEMA4 pathway, *SEMA4G-PLXNB2* and *SEMA4D-PLXNB2*, play a significant role in these processes (Supplementary Figure S11F).

Through pattern recognition analysis, detailed signaling patterns were further investigated, focusing on outgoing (ligand) and incoming (receptor) signals across these pathways (Figure 7B). Results indicated that the GC2, GC3, and GC6 clusters, located at the later stages of the pseudotime trajectory, coordinated both outgoing and incoming signals across most pathways. These findings suggest a dynamic process of GC self-regulation and interaction, with signaling activity gradually intensifying as follicular development progresses. Additionally, oocytes coordinated outgoing and incoming signals within the CD99 and LIFR pathways, significantly influencing these signaling networks (Figure 7C). Moreover, the FN1, ANGPTL, and KIT signaling pathways, primarily driven by oocytes, predominantly affected the GC2 and GC3 clusters (Figure 7D)**,** highlighting the complex signaling crosstalk between oocytes and GCs during ovarian development.

Comparative analysis of pituitary and ovarian differences between Lohmann layers and Liangshan Yanying chickens

The HPO axis plays a crucial role in regulating reproduction and egg-laying in chickens. Investigating whether the cellular heterogeneity within this axis differs between Lohmann layers and Liangshan Yanying chickens could provide valuable insights into variations in their reproductive performance and egg production. UMAP analysis revealed that cellular heterogeneity between these two chicken populations was most pronounced in the pituitary and ovary, with no significant differences observed in the hypothalamus (Figure 8A–C). Comparative assessment of cell numbers and cluster distribution further confirmed these differences in the pituitary and ovary, with minimal hypothalamic variations between the two populations (Figure 8D–F; Supplementary Figure S12A–C).

In the hypothalamus of both chicken populations, neurons were the predominant cell type, although some variations were noted in the number of cells within specific neuronal subtypes (Figure 8D; Supplementary Figure S12A). In the pituitary, distinct distribution patterns were observed across different clusters of Lac, Soma, Gona, and Pro populations, with differences in cell proportions between the two populations (Figure 8E; Supplementary Figure S12B). Specifically, the Lohmann layers displayed a higher proportion of Gona (23.60%), while the Liangshan Yanying chickens exhibited a higher proportion of Lac (30.99%). In the ovary, the primary differences between the two populations were in the proportions of various cell types, with Lohmann layers showing a higher proportion of theca cells (22.59%), stromal cells (12.79%), pre-GCs (1.37%), and GCs (21.10%), and Liangshan Yanying chickens showing a higher proportion of immune cells (Figure 8F; Supplementary Figure S12C). These differences in the distribution of cell types may significantly contribute to the variations in reproductive performance between the two chicken populations.

A comparative analysis of DEGs in the hypothalamus of the two chicken populations revealed only a small number of DEGs in neuronal cells (Supplementary Figure S12D, E and Table S5). In the pituitary, *KITLG*, known for its pleiotropic effects on cell proliferation and differentiation, exhibited differential overexpression in the Gona cells of Lohmann layers (Supplementary Figure S12F, G and Table S6). GO and KEGG analyses of these DEGs showed enrichment in terms related to “development of female primary sexual characteristics” and “female sex differentiation” (Supplementary Figure S12H, I and Tables S8, S9). In contrast, significant differences were observed in the ovary, particularly within the four functional cell types (Figure 8G, H;

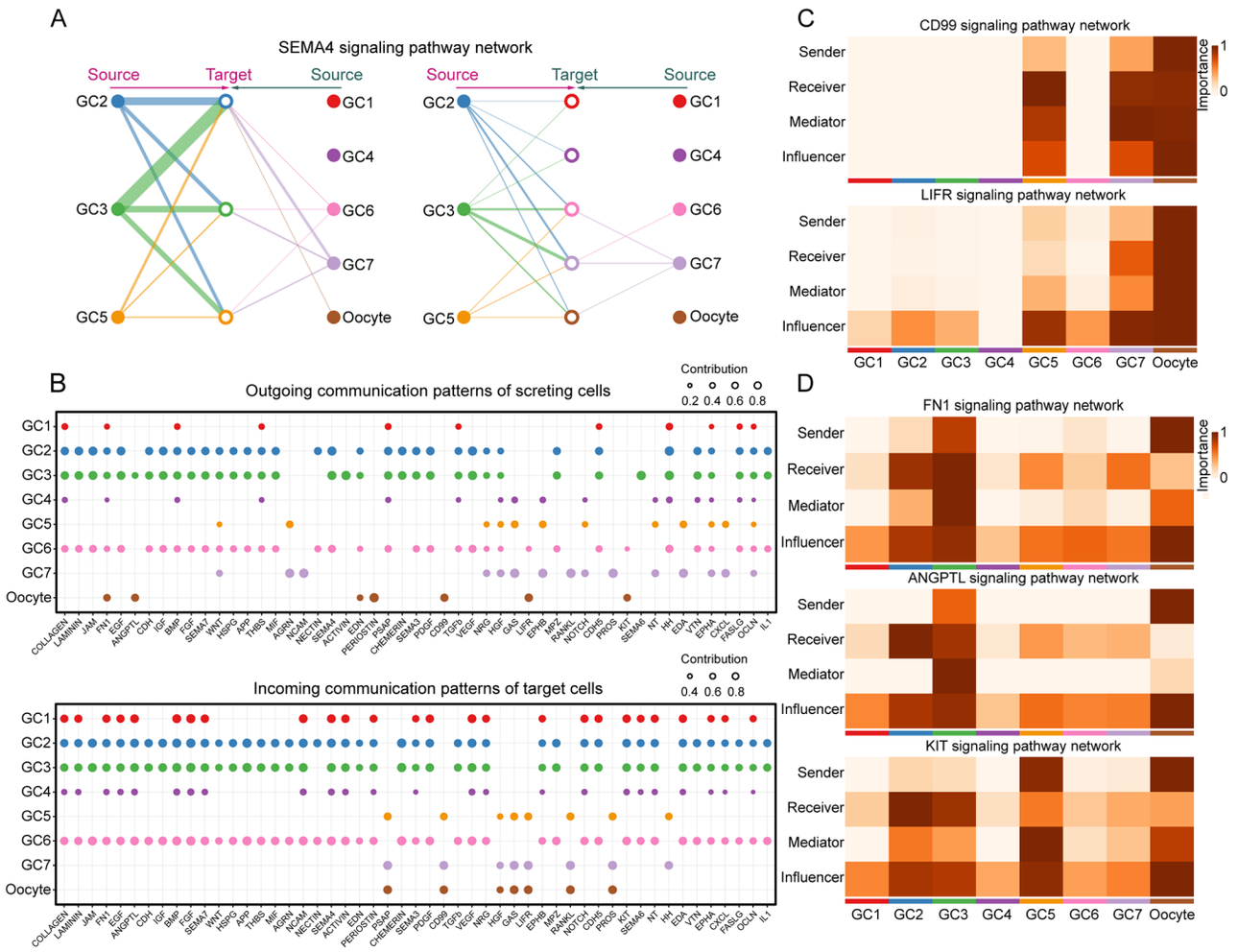

Figure 7 Signaling crosstalk between different GC subtypes and oocytes in the ovary

A: Hierarchical plot showing intercellular communication network for SEMA4 signaling pathway. Circle sizes represent number of cells, and edge widths represent communication probability. B: Dot plots showing alterations in outgoing (ligand) and incoming (receptor) signaling pathways in seven GC subtypes and oocytes. Dot size is proportional to contribution score, calculated from pattern recognition analysis. Higher contribution scores suggest that the signaling pathway is more enriched in the corresponding cell subset. C, D: Heatmap showing relative importance of each cell group based on four network centrality measures computed for CD99, LIFR, FN1, ANGPTL, and KIT signaling networks, respectively. Mediators are cells that control communication flow between any two cell groups, with higher values indicating greater capability to control communication flow. Influencers are cells that control information flow within a signaling network, with higher values indicating greater control on information flow. Importance is the magnitude of the possibility of the four roles (sender, receiver, mediator, and influencer) that cell types play. Darker colors indicate a greater role played by that cell.

Supplementary Table S7). Notably, *RLN3*, *SMAD2*, *INHBB*, and *INHA* were differentially highly expressed in the GCs of Lohmann layers (Figure 8H). GO and KEGG analyses of DEGs in GCs of Lohmann layers highlighted enrichment in terms and pathways associated with hormone synthesis and metabolism, whereas Liangshan Yanying chickens showed stronger enrichment in terms and pathways related to mitosis and the cell cycle (Figure 8I, J; Supplementary Tables S10, S11).

Further analysis of expression variations in genes related to ovarian development and function in Lohmann layers and Liangshan Yanying chickens was conducted (Figure 8K), revealing that most genes were more highly expressed in Lohmann layers. *In situ* hybridization of *GRP* and *GRPR* in the hypothalamus, pituitary, and ovary of Lohmann layers and Liangshan Yanying chickens was conducted (Supplementary Figure S13). Consistent with the sequencing data, *GRP* was mainly expressed in the anterior pituitary and partially in ovarian theca cells, while *GRPR* was mainly expressed in the hypothalamus and GCs. These findings suggest that *GRP*, primarily secreted by the pituitary Gona, may act on hypothalamic neurons through short-loop communication and on GCs of early ovarian follicles through endocrine signaling. The differential expression of *GRP* and *GRPR* in different tissues between the two chicken populations provides further evidence that *GRP* affects ovarian development in chickens. Overall, these transcript-level distinctions between Lohmann layers and Liangshan Yanying chickens across all three HPO axis tissues, particularly in the pituitary and ovary, underscore the genetic and functional divergences underlying their reproductive performance (Figure 9). Furthermore, production data collected from 100 Lohmann layers and 128 Liangshan Yanying chickens demonstrated significant differences in key reproductive traits, including body weight at the onset of laying, age at the onset of laying, and egg production at 300 days of age (Figure 8L–N).

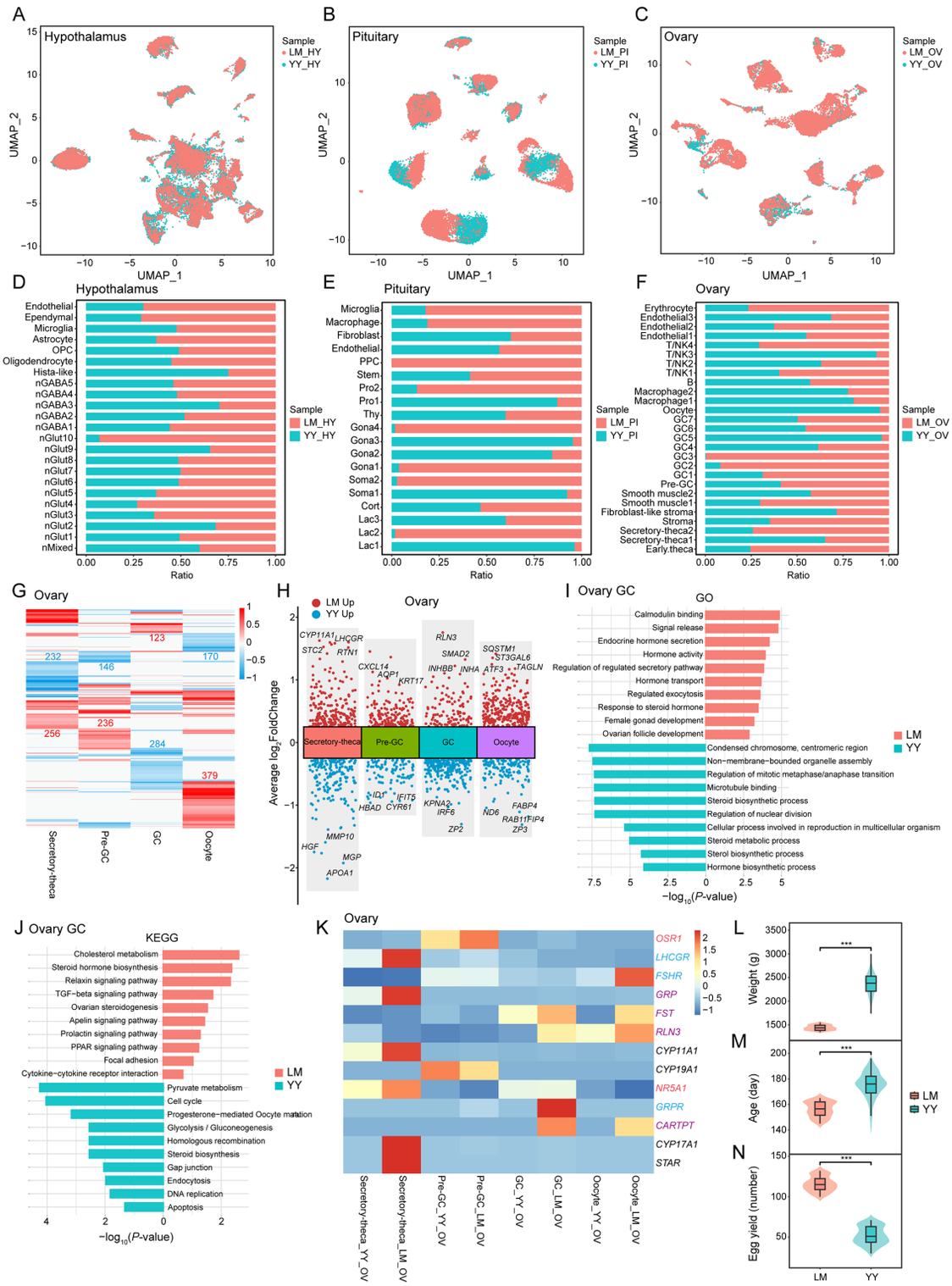

Figure 8 Differences between Lohmann layers and Liangshan Yanying chickens primarily manifested in the pituitary and ovary

A–C: UMAP plots showing distribution of all cells in the hypothalamus (HY), pituitary (PI), and ovary (OV) in different populations: Lohmann layers (LM, red) and Liangshan Yanying chickens (YY, blue). D–F: Distribution of cell numbers by cluster in the hypothalamus, pituitary, and ovary in LM and YY. Bars represent percentage of cells from LM and YY groups per cluster (0% to 100%). G: Heatmap showing DEGs in LM and YY groups in different cell types. Red and blue indicates genes up-regulated in LM and YY, respectively. Number of DEGs is indicated. H: Multiple volcano maps showing DEGs in LM and YY groups in different cell types. Representative genes are indicated. I, J: Bidirectional bar plots showing GO and KEGG enrichment analysis of DEG in GCs of LM and YY. X-axis represents *P*-value. K: Gene expression signature dividing four functional cell types of LM and YY by unsupervised hierarchical clustering. Transcription factor- (red), hormone- (purple), and receptor- (blue) related genes are marked with corresponding colors. L–N: Violin plot showing differences in weight at onset of laying, age at onset of laying, and egg production at 300 days of age between LM and YY. Box plot: median (center black line), interquartile range (dark box), and minimum-maximum range (whiskers). Wilcoxon test was used to analyze differences, with $P<0.05$ indicating a significant difference.

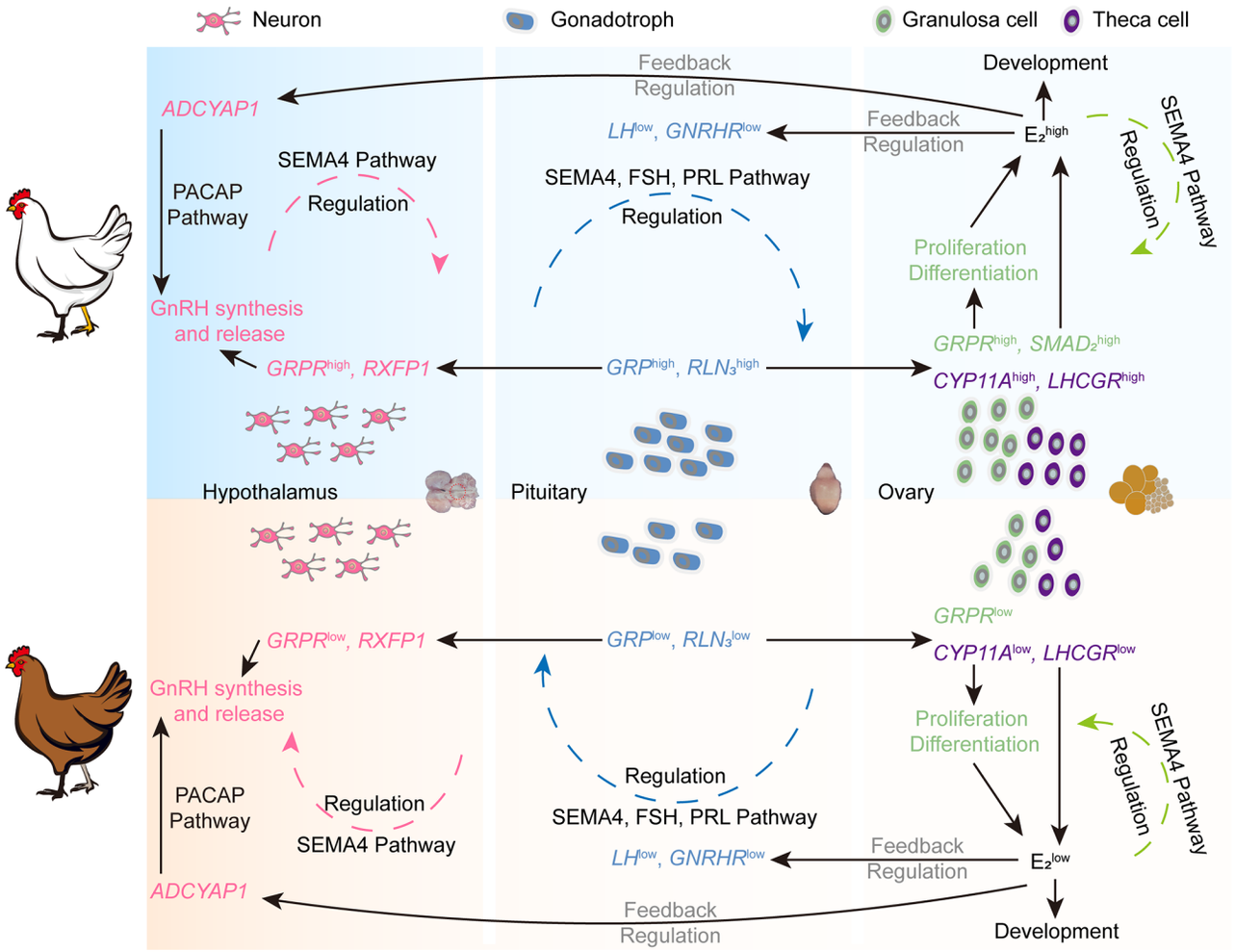

Figure 9 Schematic of HPO axis molecular network differences between Lohmann layers and Liangshan Yanying chickens

DISCUSSION

The introduction of high-resolution single-cell sequencing has revolutionized the ability to delineate the atlas of diverse cell types and determine the molecular basis underlying the cellular heterogeneity across various complex biological processes associated with physiology and pathology (Svensson et al., 2018). Despite considerable progress in this field, a comprehensive transcriptome profile encompassing all three components of the HPO axis within a single individual has not yet been fully documented. Consequently, many aspects of the intricate and highly coordinated processes within the HPO axis remain unexplored (Kaprara & Huhtaniemi, 2018; Zhao et al., 2023). In this study, we employed scRNA-seq and snRNA-seq techniques to achieve an unprecedented resolution in identifying cell type-specific molecular features in the hypothalamus, pituitary, and ovary of adult chickens. Chickens serve as a crucial model organism in biological research (Brown et al., 2003; Cogburn et al., 2007), and our investigation into the chicken HPO axis not only deepens our understanding of reproductive physiology in this species but also provides valuable insights to other species, contributing to a broader understanding of the universal mechanisms regulating the HPO axis and reproductive physiology.

Previous studies have characterized distinct cell types within the hypothalamus, pituitary, and ovarian tissues of both humans and mice. In the current investigation, we identified two prominent neuronal subtypes (nGlut and nGABA) and four glial cell subtypes in the hypothalamus of adult chickens, mirroring findings in humans and mice (Chen et al., 2017; Zhou et al., 2022). In the pituitary, we identified five classical endocrine cell populations, alongside non-endocrine cells such as stem cells and Pros. Notably, folliculostellate cells, which express the S100 protein marker and have been documented in numerous studies, were not detected in our dataset (Botermann et al., 2021; Higashi et al., 2021; Zhang et al., 2021). Additionally, while melanocyte-stimulating hormone (MSH) is typically secreted by the intermediate lobe of the pituitary in mammals, birds and other lower vertebrates lacking an intermediate lobe still contain MSH (Cal et al., 2017; El Sayed et al., 2023; Takeuchi et al., 2003; Xu et al., 2022). Nonetheless, melanotrophs were not detected in our analysis of the anterior lobe of the adult chicken pituitary, nor in previously published datasets. This absence may be attributed to the high expression of *POMC* in melanotrophs, which may prevent the formation of distinct clusters during analysis, similar to Cort (Zhang et al., 2021). In the ovary, we identified four primary cell types, including immune cells (macrophages, T/NK cells, and B cells), GCs, theca cells, and stromal cells, consistent with findings in mammals (Fan et al., 2019; Morris et al., 2022; Wang et al., 2020). However, oocytes were less abundant in our dataset. These discrepancies in captured cell types and proportions may be attributed to the heterogeneity of species, developmental processes, tissue conditions, and different sequencing

platform limitations.

The HPO axis represents a comprehensive and coordinated neuroendocrine system, essential for regulating reproductive function. The hypothalamus orchestrates the release of LH and FSH from the pituitary via the secretion of GnRH into the pituitary portal system, thereby governing ovarian development and sex hormone secretion (Spaziani et al., 2021). The synthesis and release of GnRH are affected by complex neuroregulatory mechanisms and vascular supply. Among the various ligands interacting with GnRH in the regulation of reproduction, PACAP (or ADCYAP1) plays a crucial role. Notably, PACAP modulates the effects of GnRH on gonadotropin gene expression, not only by altering hypothalamic GnRH release but also by facilitating substantial cross-talk within the pituitary, affecting receptor expression, intracellular signaling, and transcriptional regulation (Halvorson, 2014). Studies have demonstrated that the GnRH neuronal cell line, GT1-7, expresses multiple PACAP receptor splice variants and responds to PACAP stimulation by increasing cAMP production and GnRH receptor (GnRH-R) expression (Kanasaki et al., 2013; Olcese et al., 1997). Moreover, recent research has suggested a novel role for PACAP-expressing neurons in the hypothalamus, highlighting their involvement in relaying nutritional state information to regulate GnRH release, ultimately influencing reproductive function in female mice (Ross et al., 2018). In our study, the nGABA1 neuronal cluster, which predominantly expressed *GNRH1*, emerged as a major target of the PACAP signaling pathway. Conversely, the nGlut2 cluster, identified as the primary source of ligands, exhibited high expression of *ADCYAP1* and *ESR2*. These findings suggest that ovarian estrogen, acting on the hypothalamus through feedback mechanisms, may influence GnRH synthesis and release by modulating ligand production within the PACAP pathway, rather than directly acting on GnRH neurons. This insight offers potential resolution to the ongoing debate about estrogen receptor expression in GnRH neurons, suggesting new possibilities for the indirect effect of estrogen on GnRH release (Herbison & Pape, 2001; Petersen et al., 2003).

In addition, glial cells are integral to neuroendocrine regulation, participating in the transient remodeling of neuronal connections within the hypothalamus (Garcia-Segura et al., 2008). Gonadal hormones exert both direct and indirect effects on glial plasticity, modulating various signaling pathways that influence glial function and the interactions between glial cells, particularly astrocytes, and neurons (Mahesh et al., 2006; Sharif et al., 2013). The expression profiles obtained in our study revealed that different glial cells expressed distinct pituitary hormone receptors, indicating that these cells receive a variety of regulatory signals. Current research has established that glial cells interact with GnRH neurons through neurotransmitter release, endocrine regulation, signaling pathways, and environmental regulation (Clasadonte & Prevot, 2018). Our analysis identified three primary interaction pathways, including the AGT, VTN, and SEMA3 pathways. AGT is a key molecule in the renin-angiotensin system, which plays an important role in regulating blood pressure and electrolyte balance (Kahlon et al., 2022). VTN, as an extracellular matrix protein, is involved in cell adhesion and blood coagulation (Schvartz et al., 1999). SEMA3 is an important regulator involved in angiogenesis (Jiao et al., 2021). These findings suggest that, in addition to their established roles, glial cells may affect the hypothalamic environment by regulating angiogenesis and microcirculation, thereby affecting GnRH synthesis and release.

Our analysis of the pituitary dataset revealed the absence of LHB expression and minimal GNRHR expression, consistent with previous research on turkeys showing changes in HPO axis gene expression during the preovulatory surge (Brady et al., 2019, 2023). Research has demonstrated that FSH secreted in the pituitary can regulate its own secretion via a negative feedback mechanism acting on Gona (Padmanabhan & Cardoso, 2020; Ulloa-Aguirre et al., 2018). Additionally, PRL, another pituitary hormone, has been shown in many mammals to inhibit GnRH secretion from the hypothalamus. PRL can also suppress the sensitivity of pituitary Gona to GnRH under specific physiological or pathological conditions, leading to a decrease in LH secretion (Barad et al., 2020; Freeman et al., 2000; Grattan et al., 2007). Our analysis of pituitary signaling crosstalk identified Gona cells as a significant source of ligands and target cells in the FSH and PRL pathways. Furthermore, the co-expression patterns of neuropeptides and receptors in the hypothalamus suggest that growth hormone-releasing hormone (GHRH) synthesis and release in the pituitary are regulated by gonadotropins, whereas corticotropin-releasing hormone (CRH) and thyrotropin-releasing hormone (TRH) are regulated by growth hormone and estrogen, respectively. This hierarchical feedback pattern may influence the synthesis and release of GnRH and LH by regulating the secretion of PRL. We hypothesize that these regulatory mechanisms contribute to the observed alterations in gene expression within the HPO axis during the preovulatory surge. However, further research is required to determine whether these mechanisms are specific to birds or extend to other vertebrates.

Prior research has shown that *AMH* is predominantly synthesized and secreted by early follicular GCs in the ovary (Li et al., 2022; Wang et al., 2020; Zhang et al., 2018), playing a crucial role in inhibiting early follicular growth and regulating follicle number and development in the ovary (Dewailly et al., 2016; Di Clemente et al., 2021). The two primary pituitary gonadotropins, FSH and LH, stimulate *AMH* expression in small growing follicles (Dewailly et al., 2016; Di Clemente et al., 2021). In mammals, *LHCGR* is moderately expressed in the smallest follicles, and its presence is thought to be linked to the positive effects of LH on follicle survival and development (Jeppesen et al., 2012; La Marca et al., 2023). Our findings substantiate the idea that *FSHR* and *LHCGR* are highly expressed in the GC7 subtype, correlating with the highest *AMH* expression. Ovarian follicular development is a complex process involving endocrine, paracrine, and autocrine signaling within the HPO axis (Li et al., 2021). The function and gene expression profiles of GCs vary considerably during this process, facilitating follicular maturation through direct contact and adhesion to oocytes (Abbassi et al., 2021; Li et al., 2022). This complex process involves the exchange of multiple regulatory signals. Beyond the well-established KIT signaling pathway, other pathways, such as CD99, LIFR, FN1, and ANGPTL, may also participate in oocyte-GC interactions (Zhang et al., 2018). However, further experimental evidence is required to validate these potential associations.

Recent research has highlighted the significant role of RLN3 in various physiological functions, including pregnancy response, metabolism, stress regulation, and energy balance (Bathgate et al., 2013; Patil et al., 2017). RLN3 is increasingly

recognized as a novel endocrine hormone involved in female reproduction, with abundant expression in pituitary Gona cells and ovarian GCs of adult female chickens (Li et al., 2022; Zhang et al., 2021). It is also highly expressed in the hypothalamus of newly hatched chicks (Higgins et al., 2010). In this study, *RLN3* demonstrated elevated expression in hypothalamic neurons, pituitary Gona cells, and ovarian GCs. Furthermore, its receptor, *RXFP1*, co-localized with *FSHR*, *LHCGR*, and *GRPR* in neuronal clusters in the hypothalamus, suggesting complex interactions within the HPO axis. GRP and its receptor GRPR, which are conserved in vertebrates, are involved in various autonomic-related functions, such as cell growth/proliferation, circadian rhythms, emotional responses, memory, and male reproductive function (Hirooka et al., 2021; Roesler & Schwartsmann, 2012; Sakamoto et al., 2008). In chickens, *GRP* is highly expressed in the pituitary Gona cells, while *GRPR* is widely expressed in the hypothalamus and ovaries (Mo et al., 2017; Zhang et al., 2021). Consistent with these findings, our data showed high *GRP* expression in all four pituitary Gona subtypes, as well as ovarian theca cells and GCs. Conversely, *GRPR* was predominantly detected in hypothalamic neurons and ovarian GCs. CART has been detected in various tissues, including the hypothalamus, pituitary, and ovaries (Koylu et al., 1997; Li et al., 2017, 2018; Zhang et al., 2021). CART expression is tightly regulated by hypothalamic GnRH (Mo et al., 2019; True et al., 2013) and is involved in feeding regulation, ovarian follicular development, and steroidogenesis (Li et al., 2017, 2018; Venancio et al., 2017). In this study, *CARTPT* was highly expressed in hypothalamic neurons, pituitary Gona cells, and ovarian GCs. However, further research is warranted to discern the physiological implications of these findings and to explore whether RLN3, GRP, and CART function as novel endocrine hormones, contributing to the regulatory activities of the HPO axis through autocrine, paracrine, and endocrine pathways.

Semaphorin and plexins constitute a major family of guidance molecules and receptors, pivotal in processes such as cell migration, neurodevelopment, and angiogenesis (Conrotto et al., 2005; Limoni & Niquille, 2021). Within this family, semaphorin 4D (SEMA4D or CD100) serves as a crucial mediator of migration and differentiation across various cell types (Fisher et al., 2016). SEMA4D is presumed to act as both a receptor, signaling through its cytoplasmic domain, and a ligand (Hall et al., 1996). Notably, *SEMA4D* is expressed in mouse ovarian GCs, where it influences follicular development and steroid hormone secretion (Regev et al., 2007). *SEMA4D* knockout mice exhibit reduced *Gnrh1* expression in the hypothalamus and a diminished number of ovarian follicles (Dacquin et al., 2011). *SEMA4D* interacts with several cellular receptors, including *PLXNB1*, *PLXNB2*, and *CD72* (Fisher et al., 2016). Among these, *PLXNB2*, implicated in the regulation of adult cell proliferation through SEMA4D signaling, promotes the chemomigration of immortalized GnRH neurons (Giacobini et al., 2008; Saha et al., 2012). Another member of the semaphorin protein family, SEMA4G, is expressed in the mouse hypothalamus and pituitary (Li et al., 1999). Recent studies have also indicated that *SEMA4G* is highly expressed in the ovarian tissue of highly fertile goats, significantly promoting the proliferation of GCs (Chen et al., 2024). Our analysis supports the hypothesis that hypothalamic neurons, pituitary Gona cells, and ovarian GCs are the primary sources of ligands and target cells in the SEMA4 pathway, as revealed by CellChat analysis. Among the most prominent ligand-receptor pairs identified, *SEMA4D-PLXNB2* was also present in the ovary. Further research in this area should further elucidate the crucial role of the SEMA4 pathway in the regulation of the HPO axis.

In addition to cell type classification, scRNA-seq and snRNA-seq enable detailed analysis of differences in cell type proportions and gene expression within complex tissues across breeds (Verma et al., 2023). In this study, we conducted a comparative transcriptional analysis of the hypothalamus, pituitary, and ovary between Lohmann layer and Liangshan Yanying chicken populations. Overall, the primary differences between the two chicken populations were observed in the pituitary and ovary, aligning with previous transcriptome-level studies (Brady et al., 2023; Wang & Ma, 2019). Notably, the ovaries of the Lohmann layers, known for superior reproductive performance, exhibited elevated expression of three novel peptide hormones — *GRP*, *RLN3*, and *CARTPT* — along with several receptors, including *LHCGR*, *FSHR*, and *GRPR*. These findings support the hypothesis that these molecules play crucial roles in female reproduction, influencing ovarian function, follicular development, and ovulation processes. Future research on these genes in avian species and other vertebrates will not only clarify their impact on ovarian development and reproductive health in females but also their associations with diverse phenotypic traits in poultry, including egg-laying performance, reproductive strategies, body composition, and behavior.

DATA AVAILABILITY

Datasets generated in this study were deposited in the Genome Sequence Archive (GSA) database (https://ngdc.cncb.ac.cn/gsa/) (accession number CRA017114), Science Data Bank (doi:10.57760/sciencedb.09034), and NCBI (BioProjectID PRJNA947351).

SUPPLEMENTARY DATA

Supplementary data to this article can be found online.

COMPETING INTERESTS

The authors declare that they have no competing interests.

AUTHORS' CONTRIBUTIONS

D.L.: Conceptualization, Data curation, Formal analysis, Software, Validation, Visualization, Writing-original draft. B.Z.: Methodology, Software. T.W.: Writing-review & editing. B.L.C.: Funding acquisition, Investigation, Resources. D.Y.L.: Conceptualization, Funding acquisition, Methodology, Project administration, Supervision, Writing-review & editing. Z.J.L.: Supervision, Writing-review & editing. All authors read and approved the final version of the manuscript.

REFERENCES

Abbassi L, El-Hayek S, Carvalho KF, et al. 2021. Epidermal growth factor receptor signaling uncouples germ cells from the somatic follicular compartment at ovulation. *Nature Communications*, **12**(1): 1438.

Barad Z, Aung ZK, Grattan DR, et al. 2020. Impaired prolactin transport into the brain and functional responses to prolactin in aged male mice. *Journal of Neuroendocrinology*, **32**(8): e12889.

Bathgate RAD, Halls ML, Van Der Westhuizen ET, et al. 2013. Relaxin family peptides and their receptors. *Physiological Reviews*, **93**(1): 405–480.

Botermann DS, Brandes N, Frommhold A, et al. 2021. Hedgehog signaling in endocrine and folliculo-stellate cells of the adult pituitary. *Journal of Endocrinology*, **248**(3): 303–316.

Brady K, Liu HC, Hicks J, et al. 2023. Global gene expression analysis of the turkey hen hypothalamo-pituitary-gonadal axis during the preovulatory hormonal surge. *Poultry Science*, **102**(4): 102547.

Brady K, Porter TE, Liu HC, et al. 2019. Characterization of gene expression in the hypothalamo-pituitary-gonadal axis during the preovulatory surge in the turkey hen. *Poultry Science*, **98**(12): 7041–7049.

Brown WRA, Hubbard SJ, Tickle C, et al. 2003. The chicken as a model for large-scale analysis of vertebrate gene function. *Nature Reviews Genetics*, **4**(2): 87–98.

Butler A, Hoffman P, Smibert P, et al. 2018. Integrating single-cell transcriptomic data across different conditions, technologies, and species. *Nature Biotechnology*, **36**(5): 411–420.

Cal L, Suarez-Bregua P, Cerdá-Reverter JM, et al. 2017. Fish pigmentation and the melanocortin system. *Comparative Biochemistry and Physiology Part A*: *Molecular & Integrative Physiology*, **211**: 26–33.

Cao JY, Spielmann M, Qiu XJ, et al. 2019. The single-cell transcriptional landscape of mammalian organogenesis. *Nature*, **566**(7745): 496–502.

Chen RC, Wu XJ, Jiang L, et al. 2017. Single-cell RNA-Seq reveals hypothalamic cell diversity. *Cell Reports*, **18**(13): 3227–3241.

Chen XX, Sun X, Chimbaka IM, et al. 2021. Transcriptome analysis of ovarian follicles reveals potential pivotal genes associated with increased and decreased rates of chicken egg production. *Frontiers in Genetics*, **12**: 622751.

Chen YL, Wang P, He XY, et al. 2024. *SEMA4G* targeted by miR-363-5p regulates the proliferation of granulosa cells in Yunshang black goats. *Animal Research and One Health*, **2**(1): 28–38.

Clasadonte J, Prevot V. 2018. The special relationship: glia-neuron interactions in the neuroendocrine hypothalamus. *Nature Reviews Endocrinology*, **14**(1): 25–44.

Cogburn LA, Porter TE, Duclos MJ, et al. 2007. Functional genomics of the chicken--a model organism. *Poultry Science*, **86**(10): 2059–2094.

Conn PM, Crowley WF Jr. 1994. Gonadotropin-releasing hormone and its analogs. *Annual Review of Medicine*, **45**: 391–405.

Conrotto P, Valdembri D, Corso S, et al. 2005. Sema4D induces angiogenesis through Met recruitment by Plexin B1. *Blood*, **105**(11): 4321–4329.

Dacquin R, Domenget C, Kumanogoh A, et al. 2011. Control of bone resorption by semaphorin 4D is dependent on ovarian function. *PLoS One*, **6**(10): e26627.

Denef C. 2008. Paracrinicity: the story of 30 years of cellular pituitary crosstalk. *Journal of Neuroendocrinology*, **20**(1): 1–70.

Devillers MM, Mhaouty-Kodja S, Guigon CJ. 2022. Deciphering the roles & regulation of estradiol signaling during female mini-puberty: insights from mouse models. *International Journal of Molecular Sciences*, **23**(22): 13695.

Dewailly D, Robin G, Peigne M, et al. 2016. Interactions between androgens, FSH, anti-Müllerian hormone and estradiol during folliculogenesis in the human normal and polycystic ovary. *Human Reproduction Update*, **22**(6): 709–724.

Di Clemente N, Racine C, Pierre A, et al. 2021. Anti-müllerian hormone in female reproduction. *Endocrine Reviews*, **42**(6): 753–782.

Edwards W, Raetzman LT. 2018. Complex integration of intrinsic and peripheral signaling is required for pituitary gland development. *Biology of Reproduction*, **99**(3): 504–513.

El Sayed SA, Fahmy MW, Schwartz J. 2023. Physiology, pituitary gland. *In*: StatPearls. Treasure Island: StatPearls Publishing.

Estermann MA, Williams S, Hirst CE, et al. 2020. Insights into gonadal sex differentiation provided by single-cell transcriptomics in the chicken embryo. *Cell Reports*, **31**(1): 107491.

Fan X, Bialecka M, Moustakas I, et al. 2019. Single-cell reconstruction of follicular remodeling in the human adult ovary. *Nature Communications*, **10**(1): 3164.

Fisher TL, Reilly CA, Winter LA, et al. 2016. Generation and preclinical characterization of an antibody specific for SEMA4D. *mAbs*, **8**(1): 150–162.

Freeman ME, Kanyicska B, Lerant A, et al. 2000. Prolactin: structure, function, and regulation of secretion. *Physiological Reviews*, **80**(4): 1523–1631.

Garcia-Segura LM, Lorenz B, Doncarlos LL. 2008. The role of glia in the hypothalamus: implications for gonadal steroid feedback and reproductive neuroendocrine output. *Reproduction*, **135**(4): 419–429.

Giacobini P, Messina A, Morello F, et al. 2008. Semaphorin 4D regulates gonadotropin hormone-releasing hormone-1 neuronal migration through PlexinB1-Met complex. *Journal of Cell Biology*, **183**(3): 555–566.

Grattan DR, Jasoni CL, Liu XH, et al. 2007. Prolactin regulation of gonadotropin-releasing hormone neurons to suppress luteinizing hormone secretion in mice. *Endocrinology*, **148**(9): 4344–4351.

Hall KT, Boumsell L, Schultze JL, et al. 1996. Human CD100, a novel leukocyte semaphorin that promotes B-cell aggregation and differentiation. *Proceedings of the National Academy of Sciences of the United States of America*, **93**(21): 11780–11785.

Halvorson LM. 2014. PACAP modulates GnRH signaling in gonadotropes. *Molecular and Cellular Endocrinology*, **385**(1-2): 45–55.

Herbison AE, Pape JR. 2001. New evidence for estrogen receptors in gonadotropin-releasing hormone neurons. *Frontiers in Neuroendocrinology*, **22**(4): 292–308.

Higashi AY, Higashi T, Furuse K, et al. 2021. Claudin-9 constitutes tight junctions of folliculo-stellate cells in the anterior pituitary gland. *Scientific Reports*, **11**(1): 21642.

Higgins SE, Ellestad LE, Trakooljul N, et al. 2010. Transcriptional and pathway analysis in the hypothalamus of newly hatched chicks during fasting and delayed feeding. *BMC Genomics*, **11**(1): 162.

Hirooka A, Hamada M, Fujiyama D, et al. 2021. The gastrin-releasing peptide/bombesin system revisited by a reverse-evolutionary study considering *Xenopus*. *Scientific Reports*, **11**(1): 13315.

Hsueh AJW, Kawamura K, Cheng Y, et al. 2015. Intraovarian control of early folliculogenesis. *Endocrine Reviews*, **36**(1): 1–24.

Jeppesen JV, Kristensen SG, Nielsen ME, et al. 2012. LH-receptor gene expression in human granulosa and cumulus cells from antral and preovulatory follicles. *The Journal of Clinical Endocrinology & Metabolism*, **97**(8): e1524–e1531.

Jiao B, Liu SY, Tan X, et al. 2021. Class-3 semaphorins: Potent multifunctional modulators for angiogenesis-associated diseases. *Biomedicine & Pharmacotherapy*, **137**: 111329.

Jin SQ, Guerrero-Juarez CF, Zhang LH, et al. 2021. Inference and analysis of cell-cell communication using CellChat. *Nature Communications*, **12**(1): 1088.

Johnson AL. 2015. Ovarian follicle selection and granulosa cell differentiation. *Poultry Science*, **94**(4): 781–785.

Kahlon T, Carlisle S, Mostacero DO, et al. 2022. Angiotensinogen: more than its downstream products: evidence from population studies and novel therapeutics. *JACC: Heart Failure*, **10**(10): 699–713.

Kanasaki H, Mijiddorj T, Sukhbaatar U, et al. 2013. Pituitary adenylate cyclase-activating polypeptide (PACAP) increases expression of the gonadotropin-releasing hormone (GnRH) receptor in GnRH-producing GT1-7 cells overexpressing PACAP type I receptor. *General and Comparative Endocrinology*, **193**: 95–102.

Kaprara A, Huhtaniemi IT. 2018. The hypothalamus-pituitary-gonad axis: Tales of mice and men. *Metabolism*, **86**: 3–17.

Kim DW, Place E, Chinnaiya K, et al. 2022. Single-cell analysis of early chick hypothalamic development reveals that hypothalamic cells are induced from prethalamic-like progenitors. *Cell Reports*, **38**(3): 110251.

Koylu EO, Couceyro PR, Lambert PD, et al. 1997. Immunohistochemical localization of novel CART peptides in rat hypothalamus, pituitary and

adrenal gland. *Journal of Neuroendocrinology*, **9**(11): 823–833.
La Marca A, Longo M, Sighinolfi G, et al. 2023. New insights into the role of LH in early ovarian follicular growth: a possible tool to optimize follicular recruitment. *Reproductive BioMedicine Online*, **47**(6): 103369.
Le Tissier PR, Hodson DJ, Lafont C, et al. 2012. Anterior pituitary cell networks. *Frontiers in Neuroendocrinology*, **33**(3): 252–266.
Li DY, Ning CY, Zhang JM, et al. 2022. Dynamic transcriptome and chromatin architecture in granulosa cells during chicken folliculogenesis. *Nature Communications*, **13**(1): 131.
Li HZ, Wu DK, Sullivan SL. 1999. Characterization and expression of *sema4g*, a novel member of the semaphorin gene family. *Mechanisms of Development*, **87**(1-2): 169–173.
Li LY, Shi XJ, Shi Y, et al. 2021. The signaling pathways involved in ovarian follicle development. *Frontiers in Physiology*, **12**: 730196.
Li PF, Meng JZ, Jing JJ, et al. 2018. Study on the relationship between expression patterns of cocaine-and amphetamine regulated transcript and hormones secretion in porcine ovarian follicles. *Biological Research*, **51**(1): 6.
Li PF, Yu XJ, Xie JS, et al. 2017. Expression of cocaine- and amphetamine-regulated transcript (CART) in hen ovary. *Biological Research*, **50**(1): 18.
Li R, Albertini DF. 2013. The road to maturation: somatic cell interaction and self-organization of the mammalian oocyte. *Nature Reviews Molecular Cell Biology*, **14**(3): 141–152.
Limoni G, Niquille M. 2021. Semaphorins and Plexins in central nervous system patterning: the key to it all?. *Current Opinion in Neurobiology*, **66**: 224–232.
Lopez JP, Brivio E, Santambrogio A, et al. 2021. Single-cell molecular profiling of all three components of the HPA axis reveals adrenal ABCB1 as a regulator of stress adaptation. *Science Advances*, **7**(5): eabe4497.
Ludwig CLM, Bohleber S, Lapp R, et al. 2023. Alterations in gonadotropin, apoptotic and metabolic pathways in granulosa cells warrant superior fertility of the Dummerstorf high fertility mouse line 1. *Journal of Ovarian Research*, **16**(1): 32.
Maggi R, Cariboni AM, Marelli MM, et al. 2016. GnRH and GnRH receptors in the pathophysiology of the human female reproductive system. *Human Reproduction Update*, **22**(3): 358–381.
Mahesh VB, Dhandapani KM, Brann DW. 2006. Role of astrocytes in reproduction and neuroprotection. *Molecular and Cellular Endocrinology*, **246**(1-2): 1–9.
McInnes L, Healy J, Saul N, et al. 2018. UMAP: uniform manifold approximation and projection. *Journal of Open Source Software*, **3**(29): 861.
Mikhael S, Punjala-Patel A, Gavrilova-Jordan L. 2019. Hypothalamic-pituitary-ovarian axis disorders impacting female fertility. *Biomedicines*, **7**(1): 5.
Millar RP. 2005. GnRHs and GnRH receptors. *Animal Reproduction Science*, **88**(1-2): 5–28.
Mo CH, Huang L, Cui L, et al. 2017. Characterization of NMB, GRP and their receptors (BRS3, NMBR and GRPR) in chickens. *Journal of Molecular Endocrinology*, **59**(1): 61–79.
Mo CH, Lv C, Huang L, et al. 2019. Regulation of pituitary cocaine- and amphetamine-regulated transcript expression and secretion by hypothalamic gonadotropin-releasing hormone in chickens. *Frontiers in Physiology*, **10**: 882.
Morris ME, Meinsohn MC, Chauvin M, et al. 2022. A single-cell atlas of the cycling murine ovary. *eLife*, **11**: e77239.
Olcese J, McArdle CA, Middendorff R, et al. 1997. Pituitary adenylate cyclase-activating peptide and vasoactive intestinal peptide receptor expression in immortalized LHRH neurons. *Journal of Neuroendocrinology*, **9**(12): 937–943.
Padmanabhan V, Cardoso RC. 2020. Neuroendocrine, autocrine, and paracrine control of follicle-stimulating hormone secretion. *Molecular and Cellular Endocrinology*, **500**: 110632.
Patil NA, Rosengren KJ, Separovic F, et al. 2017. Relaxin family peptides: structure-activity relationship studies. *British Journal of Pharmacology*, **174**(10): 950–961.
Perez-Castro C, Renner U, Haedo MR, et al. 2012. Cellular and molecular specificity of pituitary gland physiology. *Physiological Reviews*, **92**(1): 1–38.
Petersen SL, Ottem EN, Carpenter CD. 2003. Direct and indirect regulation of gonadotropin-releasing hormone neurons by estradiol. *Biology of Reproduction*, **69**(6): 1771–1778.
Regev A, Goldman S, Shalev E. 2007. Semaphorin-4D (Sema-4D), the Plexin-B1 ligand, is involved in mouse ovary follicular development. *Reproductive Biology and Endocrinology*, **5**(1): 12.
Roesler R, Schwartsmann G. 2012. Gastrin-releasing peptide receptors in the central nervous system: role in brain function and as a drug target. *Frontiers in Endocrinology*, **3**: 159.
Ross RA, Leon S, Madara JC, et al. 2018. PACAP neurons in the ventral premammillary nucleus regulate reproductive function in the female mouse. *eLife*, **7**: e35960.
Saha B, Ypsilanti AR, Boutin C, et al. 2012. Plexin-B2 regulates the proliferation and migration of neuroblasts in the postnatal and adult subventricular zone. *Journal of Neuroscience*, **32**(47): 16892–16905.
Sakamoto H, Matsuda KI, Zuloaga DG, et al. 2008. Sexually dimorphic gastrin releasing peptide system in the spinal cord controls male reproductive functions. *Nature Neuroscience*, **11**(6): 634–636.
Santiago-Andres Y, Golan M, Fiordelisio T. 2021. Functional pituitary networks in vertebrates. *Frontiers in Endocrinology*, **11**: 619352.
Schvartz I, Seger D, Shaltiel S. 1999. Vitronectin. *The International Journal of Biochemistry & Cell Biology*, **31**(5): 539–544.
Sharif A, Baroncini M, Prevot V. 2013. Role of glia in the regulation of gonadotropin-releasing hormone neuronal activity and secretion. *Neuroendocrinology*, **98**(1): 1–15.
Spaziani M, Tarantino C, Tahani N, et al. 2021. Hypothalamo-Pituitary axis and puberty. *Molecular and Cellular Endocrinology*, **520**: 111094.
Sun X, Zhu HY, Zhang CY, et al. 2023. Transcriptomic analysis of ovarian follicles uncovers the crucial genes relevant to follicle selection and preovulatory hierarchy in hens. *Journal of Animal Science*, **101**: skad241.
Svensson V, Vento-Tormo R, Teichmann SA. 2018. Exponential scaling of single-cell RNA-seq in the past decade. *Nature Protocols*, **13**(4): 599–604.
Takeuchi S, Takahashi S, Okimoto R, et al. 2003. Avian melanocortin system: α-MSH may act as an autocrine/paracrine hormone: a minireview. *Annals of the New York Academy of Sciences*, **994**(1): 366–372.
True C, Verma S, Grove KL, et al. 2013. Cocaine- and amphetamine-regulated transcript is a potent stimulator of GnRH and kisspeptin cells and may contribute to negative energy balance-induced reproductive inhibition in females. *Endocrinology*, **154**(8): 2821–2832.
Ulloa-Aguirre A, Reiter E, Crépieux P. 2018. FSH receptor signaling: complexity of interactions and signal diversity. *Endocrinology*, **159**(8): 3020–3035.
Venancio JC, Margatho LO, Rorato R, et al. 2017. Short-term high-fat diet increases leptin activation of CART neurons and advances puberty in female mice. *Endocrinology*, **158**(11): 3929–3942.
Verma R, Sahu P, Rana A, et al. 2023. Single cell RNA-sequencing and its application in livestock animals. *Systems Biology, Bioinformatics and Livestock Science*, **1**(1): 226–242.
Wang CQ, Ma W. 2019. Hypothalamic and pituitary transcriptome profiling using RNA-sequencing in high-yielding and low-yielding laying hens. *Scientific Reports*, **9**(1): 10285.
Wang S, Zheng YX, Li JY, et al. 2020. Single-cell transcriptomic atlas of primate ovarian aging. *Cell*, **180**(3): 585–600. e19.
Wang ZY, E GX, Liu CB, et al. 2023. Comparative transcriptomic profiling in ovarian tissues of lohmann hens and Chengkou mountain chicken.

Frontiers in Bioscience-Landmark, **28**(10): 267.

Wu TZ, Hu EQ, Xu SB, et al. 2021. clusterProfiler 4.0: A universal enrichment tool for interpreting omics data. *The Innovation*, **2**(3): 100141.

Xu YL, Yan JX, Tao Y, et al. 2022. Pituitary hormone α-MSH promotes tumor-induced myelopoiesis and immunosuppression. *Science*, **377**(6610): 1085–1091.

Zappia L, Oshlack A. 2018. Clustering trees: a visualization for evaluating clusterings at multiple resolutions. *GigaScience*, **7**(7): giy083.

Zhang JN, Lv C, Mo CH, et al. 2021. Single-cell RNA sequencing analysis of chicken anterior pituitary: a bird's-eye view on vertebrate pituitary. *Frontiers in Physiology*, **12**: 562817.

Zhang S, Cui YL, Ma XY, et al. 2020. Single-cell transcriptomics identifies divergent developmental lineage trajectories during human pituitary development. *Nature Communications*, **11**(1): 5275.

Zhang YY, Yan ZQ, Qin QY, et al. 2018. Transcriptome landscape of human folliculogenesis reveals oocyte and granulosa cell interactions. *Molecular Cell*, **72**(6): 1021–1034. e4.

Zhao JB, Pan HB, Liu Y, et al. 2023. Interacting networks of the hypothalamic-pituitary-ovarian axis regulate layer hens performance. *Genes*, **14**(1): 141.

Zhou X, Lu YF, Zhao FQ, et al. 2022. Deciphering the spatial-temporal transcriptional landscape of human hypothalamus development. *Cell Stem Cell*, **29**(2): 328–343. e5.

Zhu XY, Gleiberman AS, Rosenfeld MG. 2007. Molecular physiology of pituitary development: signaling and transcriptional networks. *Physiological Reviews*, **87**(3): 933–963.